Journal Pre-proof

Experimental study of water-extractable sulphate in Opalinus Clay and implications for deriving porewater concentrations

Lukas Aschwanden, Paul Wersin, Mathieu Debure, Daniel Traber

PII: S0883-2927(23)00282-2

DOI: https://doi.org/10.1016/j.apgeochem.2023.105837

Reference: AG 105837

To appear in: *Applied Geochemistry*

Received Date: 20 February 2023

Revised Date: 11 July 2023

Accepted Date: 8 November 2023

Please cite this article as: Aschwanden, L., Wersin, P., Debure, M., Traber, D., Experimental study of water-extractable sulphate in Opalinus Clay and implications for deriving porewater concentrations, *Applied Geochemistry* (2023), doi: https://doi.org/10.1016/j.apgeochem.2023.105837.

Experimental study of water-extractable sulphate in Opalinus Clay and implications for deriving porewater concentrations

Lukas Aschwanden[1*], Paul Wersin[1], Mathieu Debure[2] and Daniel Traber[3]

[1]*Rock-Water Interaction, Institute of Geological Sciences, University of Bern, Baltzerstrasse 1–3, 3012 Bern, Switzerland*

[2]*BRGM, French Geological Survey, 3 av. Claude-Guillemin, 45060 Orléans, France*

[3]*NAGRA, National Cooperative for the Disposal of Radioactive Waste, Hardstrasse 73, 5430 Wettingen, Switzerland*

[*]Corresponding author: lukas.aschwanden@geo.unibe.ch

Keywords: Excess sulphate, aqueous extraction, Opalinus Clay, porewater

Abstract

In northern Switzerland, the Opalinus Clay, a Jurassic claystone formation, is foreseen as host rock for a deep geological repository for radioactive waste. Characterizing its porewater is of particular importance for assessing the mobility of radionuclides and the stability of the engineered barriers. Although the porewater composition of the Opalinus Clay is fairly well known, there is still controversy on the sources of sulphate obtained by different porewater characterization methods. A striking observation is that sulphate concentrations from aqueous extraction and recalculated to in-situ conditions are consistently much higher than sulphate concentrations measured in borehole waters, squeezed waters and advectively displaced waters ("excess sulphate"). Accordingly, the main objective of this study is to better investigate the processes affecting dissolved sulphate concentrations during aqueous extraction and, thus, to reduce uncertainties in predicting the concentrations of this compound in the Opalinus Clay porewater. To this end, a series of extraction experiments were conducted using variable solid/liquid ratios, extraction times and extract solutions. In order to suppress sulphide-mineral oxidation, all the experiments were performed in a glovebox under oxygen-free conditions (atmosphere and solutions). Measurements of the sulphur and oxygen isotope composition of the dissolved sulphate in aqueous extracts are aimed to further constrain the source of the "excess sulphate". Finally, the plausibility of the SO_4 data from extraction experiments in terms of their representativeness for in-situ conditions was evaluated by simple geochemical modelling. The modelling shows that SO_4 concentrations

from aqueous extracts recalculated to in-situ conditions imply dissolved and exchangeable cation concentrations which are not consistent with measured data, thus, attesting non-conservative behaviour for sulphate during aqueous extraction. However, the various extraction experiments showed that pyrite oxidation was successfully suppressed during the experiments and neither contributions from e.g. organic material, congruent calcite dissolution and/or sulphate mineral dissolution provide enough SO_4 to explain the "excess sulphate". Ultimately, the various extraction experiments failed to definitely identify the source of the "excess sulphate" in aqueous extracts. However, the good agreement found between the $\delta^{18}O$ and $\delta^{34}S$ values of dissolved SO_4 in aqueous extracts and those of borehole waters suggest that the "excess sulphate" might be weakly bound to mineral surfaces.

1 Introduction

In northern Switzerland, the Opalinus Clay (OPA), a Jurassic (early Aalenian) claystone formation, is foreseen as host rock for a deep geological repository for radioactive waste. Since the last 30 years Nagra – the Swiss National Cooperative for the Disposal of Radioactive Waste – and several partner organizations have been carrying out an extensive site and host rock investigation program that aims at selecting a suitable site for a deep geological repository. An important aspect of this program refers to characterizing the porewater of the Opalinus Clay, which is of particular importance for assessing the mobility of radionuclides and the efficiency of the technical barriers - i.e. the bentonite tunnel backfill or carbon steel canisters in which the radioactive waste is stored (Nagra, 2002). For example, it is conceivable that, following repository closure, once anaerobic conditions re-established, microbial reduction of dissolved sulphate and associated production of sulphide could occur in some locations (e.g. in the excavation disturbed zone surrounding the emplacement tunnels). This could increase sulphide diffusion to the canisters, and possibly affect corrosion (e.g. Pekala et al., 2020). Accordingly, knowledge on the inventory of the dissolved sulphate and the processes that control its concentration in the porewater of the Opalinus Clay is of particular importance for the design of the technical barriers.

Although the porewater composition of the OPA is fairly well known (Pearson et al., 2003; Wersin et al., 2013; Waber & Rufer 2017; Wersin et al., 2020; Wersin et al., 2022), there is still controversy on the sources of sulphate in different porewater characterisation methods. A striking observation is that sulphate concentrations obtained by aqueous extraction and recalculated to in-situ conditions are consistently much higher than sulphate concentrations

measured in borehole waters or in squeezed waters and advectively displaced waters (i.e. "excess sulphate"; Wersin et al., 2013; Waber & Rufer 2017; Wersin et al., 2020). This is illustrated in Fig. 1, which shows the profiles of chloride and sulphate concentrations in the Opalinus Clay porewater across the Mont Terri Rock Laboratory obtained by the different sampling methods. For chloride – a conservative anion (see below) – there is good agreement between the different methods. Mazurek et al. (2011) modelled the profile of chloride (and other tracers) by 1D diffusive exchange with the bounding aquifers and showed that the asymmetric curved shape of the profile can be explained by diffusion only. Regarding sulphate, squeezed and borehole waters also show consistent concentrations, however, in-situ sulphate concentrations of the porewater recalculated from aqueous extraction are distinctly higher. Methodological differences regarding porewater sulphate concentrations are not only observed for the Opalinus Clay but also for other claystones currently being investigated in the context of radioactive waste disposal, such as the Callovo-Oxfordian claystones at Bure in France (Gaucher et al. 2009) or for Boom Clay at Mol in Belgium (De Craen et al. 2004).

In contrast to high-pressure squeezing (Mazurek et al., 2015 and references therein) and advective displacement (Mäder, 2018) where the porewater is directly extracted from the rock, aqueous extraction constitutes a technique for indirect porewater characterisation. The basic principle of the method is to immerse a known mass of water-saturated rock into a known volume of ultra-pure water for a specific amount of time during which the system re-equilibrates. Thus, the solutes in aqueous extracts originate from different potential sources: 1) constituents originally dissolved in the porewater, 2) induced mineral dissolution and precipitation, cation exchange and sorption reactions during the extraction test, and 3) possibly minor contributions from fluid inclusions in minerals (i.e. small quantities of diagenetic fluid trapped within a mineral during its growth). Accordingly, conversion of solute concentrations measured in aqueous extracts to porewater solute concentrations can only be applied for ions that are not involved in any reactions - i.e., that behave conservatively - and for which the only source is the porewater. For the Opalinus Clay these conditions are met for the anions Cl and Br (Waber et al., 2003; Wersin et al. 2013, Waber & Rufer 2017, Wersin et al., 2020), whereas all other anions and cations are, to variable degrees, involved in mineral reactions. For sulphate, for example, oxidation of pyrite before and/or during the aqueous leaching experiments would obviously explain the observed difference. However, the drillcore samples used for extraction experiments were vacuum-sealed immediately after core recovery and the experiments were conducted in a glovebox – i.e. under oxygen-free conditions. Thus, pyrite oxidation is not considered plausible.

Alternatively, dissolution of a sulphate phase, such as diagenetic anhydrite or gypsum in addition to the porewater sulphate could control sulphate concentrations in the aqueous extracts. However, despite of the extensive mineralogical characterization of the Opalinus Clay (Pearson et al. 2003, Lerouge et al. 2014, Pekala et al. 2018, Jenni et al. 2019, Mazurek et al. 2023) no occurrences of diagenetic anhydrite or gypsum have been reported. Moreover, porewaters, as sampled in boreholes and squeezed waters, generally indicate undersaturation with respect to these minerals (Wersin et al. 2020; some exceptions reported in Kizcka et al. 2023). Alternatively, Wersin et al. (2013) suggest that dissolution of celestite ($SrSO_4$) or barite ($BaSO_4$), which have been identified as trace phases in the Opalinus Clay (e.g. Lerouge et al. 2014), could control sulphate concentrations in the aqueous extracts. Considering that borehole waters, squeezed waters and waters extracted by advective displacement are close to equilibrium with respect to celestite, this seemingly is a viable hypothesis. Gaucher et al. (2009) uses a similar hypothesis for explaining the observed sulphate levels in aqueous extracts of the Callovo-Oxfordian claystones at Bure.

On the other hand, a spectroscopic study by Jenni et al. (2019) found that – apart from pyrite – the sulphur inventory in the Opalinus Clay is dominated by calcite and apatite, whereas the contribution of celestite is of lesser quantitative importance. Both calcite and apatite can incorporate sulphur (or sulphate) as trace constituent, however, neither the mode of incorporation nor its structural position is exactly known (Fichtner et al., 2017).

As a third option, sulphur associated with organic matter could also play a role (Wersin et al. 2013). However, all these hypotheses have never been specifically tested in extraction experiments. Accordingly, the main objective of this study is to better investigate the processes affecting dissolved sulphate concentrations during aqueous extraction and, thus, to reduce uncertainties in predicting the concentrations of this compound in OPA porewater. For the extraction experiments, a set of seven drillcore samples from the Opalinus Clay was tested using different solid/liquid (S/L) ratios, sample masses, extraction times, preparation methods (i.e. crushed vs. milled material) and extract solutions. Moreover, $\delta^{34}S$ and $\delta^{18}O$ of dissolved sulphate in extract solutions and borehole water were measured. Finally, geochemical modelling based on cation exchange data, which constitutes an independent dataset, was performed in order to assess the plausibility of the two variants for SO_4 concentrations in the porewater of the Opalinus Clay obtained from the different characterization methods (i.e. high-SO_4 variant by aqueous extraction versus low-SO_4 variant by advective displacement, high-pressure squeezing and borehole waters).

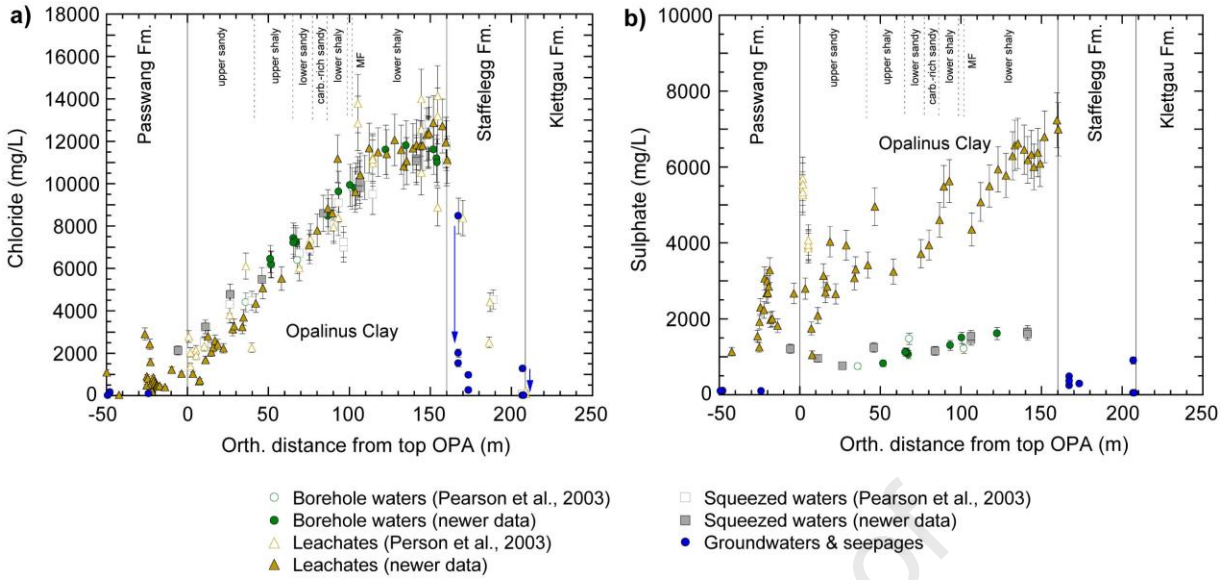

Fig. 1: a) Chloride and b) sulphate profile from the Mont Terri Underground Rock Laboratory for squeezed, borehole and seepage waters in comparison with data from aqueous extracts (modified after Wersin et al., 2020). Anion concentrations from aqueous extraction are recalculated to in-situ conditions using an anion-accessible porosity fraction of 0.54 (Person et al., 2003).

2 Sample description

A total of seven drillcore samples from the Opalinus Clay were investigated in this study. The mineralogical composition of the Opalinus Clay is well known. According to the rock parameter database compiled by Mazurek (2017) the main mineral fractions of the Opalinus Clay are (in wt.% ± 1σ): clay minerals (52.9 ± 14.9), quartz (21.4 ± 9.6) calcite (18.2 ± 11.7) and feldspars (3.3 ± 2.2). The clay minerals in the fraction <2 µm include mainly illite, illite/smectite mixed layers and kaolinite, whereas chlorite contents are subordinate. Pyrite and organic matter are ubiquitous (<0.1 – 2.0 wt.% and 0.5 – 1.5 wt.%, respectively). Moreover, accessory minerals are present, which are commonly not identified by X-ray diffraction. For example, diagenetic celestite and Ba-Sr sulphate have been detected at instances by microscopic techniques, usually as large grains (> 100 µm; Wersin et al. 2013; Lerouge et al., 2014; Lerouge et al., 2015; Pekala et al. 2018). Based on electron microscopy and X-ray spectroscopy Jenni et al. (2019) also found indications for small amounts (<0.047 g/kg $_{dry\ rock}$) of sub-µm-sized celestite grains finely disseminated in the rock matrix. In addition, sulphate associated with calcite is also present and constitutes a larger sulphate pool (<0.84 g/kg $_{dry\ rock}$). No other diagenetic sulphate minerals have been identified in the rock matrix of the Opalinus Clay, despite extensive mineralogical investigations (Pearson et al. 2003, Lerouge et al. 2014, Pekala et al. 2018, Jenni et al. 2019, Mazurek et al., 2023).

Five of the investigated drillcore samples are from the Mont Terri Rock Laboratory – an important international underground research facility for deep geological disposal of radioactive waste (Pearson et al., 2003). It is situated to the north of St-Ursanne in the canton of Jura, Switzerland (Fig. 2a) approximately 300 m underground and comprises around 1200 m of tunnels and niches for experiments. The samples were retrieved from three different boreholes: 1) from the BCI-21 borehole at depths of 3.05 m and 5.75 m from the tunnel floor (samples BCI-21A-290-319 and BCI-21-550-600, respectively), 2) from the BCS-7 borehole at 10.5 m depth (sample BCS-7) and 3) from the BPF1 borehole at depths of 3.90 m and 4.30 m (samples BPF1-3.90 and BPF1-4.30, respectively).

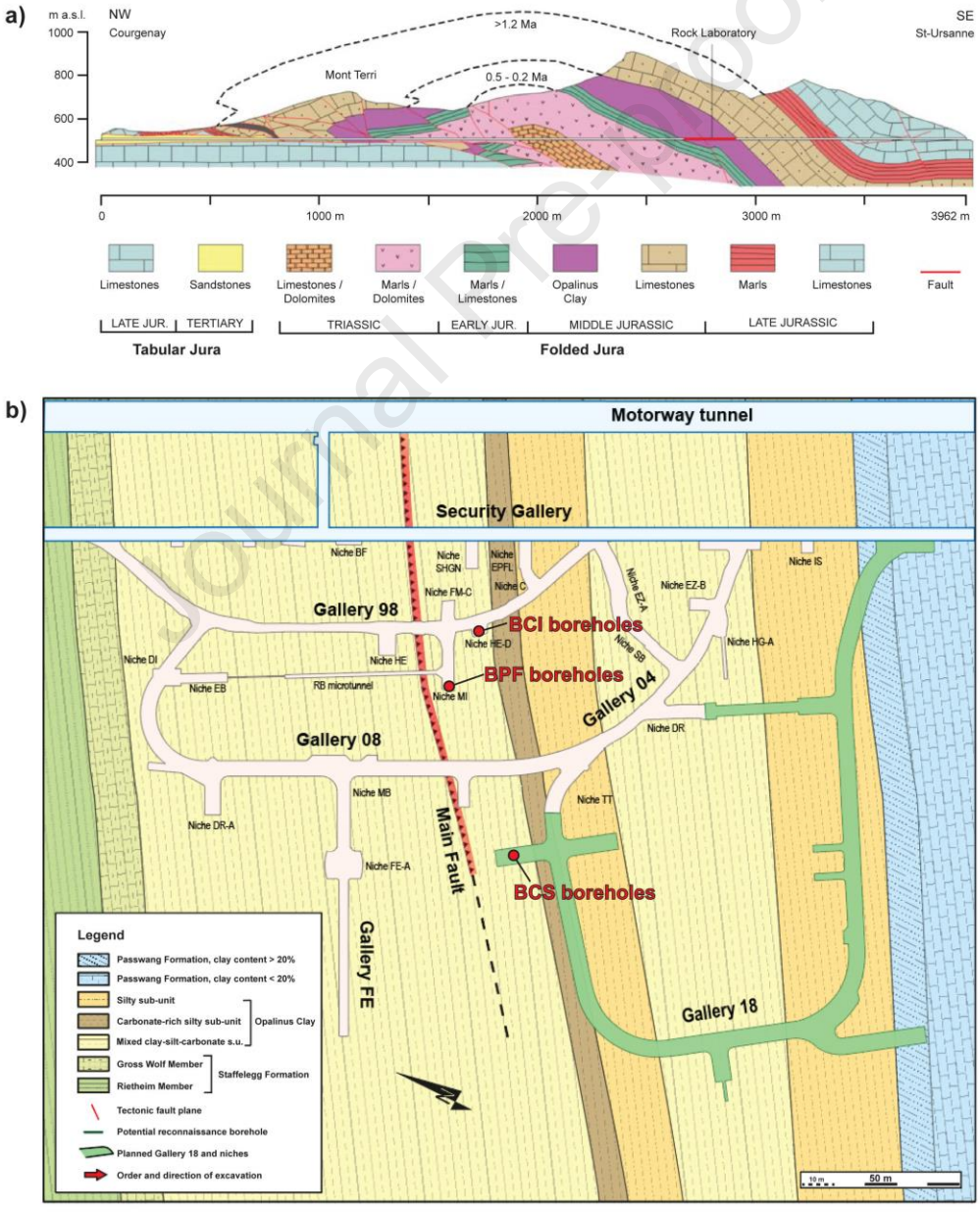

Fig. 2: a) Geological Profile across the Mont Terri anticline and location of the underground rock laboratory. Schematic representation of the erosion history (modified after Freivogel and Huggenberger, 2003). b) Map view of the Mont Terri Underground Rock Laboratory with location of boreholes (borehole mouth) from which drillcore samples were extracted for the present study (modified from map provided by D. Jäggi, Swiss Federal Office of Topography swisstopo).

The other two samples investigated in this study are from the Bülach-1-1 borehole (BUL1-1-858.60-RP and BUL1-1-909.24-RP) - an exploratory borehole drilled by Nagra in 2019 - situated between the villages of Glattfelden and Bülach (18 km to the north of the city of Zürich; for details see Mazurek et al., 2021).

3 Methods

The extraction experiments performed in this study involved 1) aqueous extraction at different solid/liquid (S/L) ratios, sample masses, extraction times and preparation methods (i.e. crushed vs. milled material) for identifying potential experimental artefacts, 2) sequential aqueous extracts in order to provide quantitative information on the inventory and the potential release of SO_4 during the experiments, 3) measurements of organic carbon in aqueous extracts to identify potentially associated SO_4 contributions, 4) nickel-ethylenediamine extracts for determining the exchangeable cation population and the total inventories of Sr and Ba and 5) acid extractions for specifically addressing the question of SO_4 released from the carbonate fraction. Moreover, analyses of $\delta^{34}S$ and $\delta^{18}O$ of dissolved sulphate in aqueous extracts and borehole water are aimed to better constrain the processes controlling sulphate concentrations in aqueous extracts.

The extraction experiments were performed at two different laboratories, at the Institute of Geological Sciences, University of Bern, Switzerland and at the French Geological Survey (BRGM), Orléans, France. Methodological details are described in the following subsections. Apart from the various extraction experiments and isotope measurements the analytical program also involves determination of the rock properties such as the gravimetric water content and the bulk-rock mineralogy by X-ray diffraction (XRD) and CNS analyser (elemental contents of inorganic and organic carbon and total sulphur). These standard techniques follow the general principles described by Waber and Rufer (2017) and Wersin et al. (2020) and are not further detailed here.

3.1 Sample preparation for extraction experiments and experimental conditions

The fundamental principle of porewater investigations relies on preserving the initial state of the drillcore samples upon recovery by minimizing their desiccation, oxidation and outgassing by sealing into evacuated and gas-tight bags (PET-Aluminium-Polyethylene compound foil) on-site, immediately after core recovery. For experiments performed at the University of Bern the samples were rapidly unpacked in the lab (under atmospheric conditions) where the rim as well as the bottom and top part of the drillcore samples were trimmed off (1.5 cm; potentially contaminated by the drilling fluid and pre-exposed to the atmosphere). The central rock material was disintegrated to 0.5–1 cm sized fragments, of which a subsample was milled with a tungsten carbide disc mill (120 s at 720 rpm; <63 µm grain size). Crushed and milled material were then transferred into a glovebox where the extraction experiments were performed under anaerobic conditions (pO_2 <1 ppm). The preparation time under atmospheric conditions – i.e. from unpacking the samples until transfer into the glovebox – was minimized to <8 minutes to suppress sulphide mineral oxidation and porewater evaporation as much as possible. For experiments performed at BRGM the entire process of sample preparation was performed in a glovebox at fixed N_2 and CO_2 levels. The sample rims were also removed and the central rock material was freeze-dried. The freeze-dried sample was then split into two batches: one was grinded and sieved (<63 µm grain size), the other was crushed to 0.5–1 cm sized fragments.

3.2 Aqueous extracts

The aqueous extraction experiments performed at the University of Bern followed the general procedures described by Waber and Rufer (2017). Experiments performed by BRGM followed the methodology described by Debure et al. (2018). Generally, degassed oxygen- and CO_2-free ultra-pure water was used for the extractions. The experiments involved numerous tests at variable S/L ratios (0.05–1 g/mL), extraction times (0.2–168 h) and using crushed and milled material. Note that milling reduces the grain size and opens fluid inclusions that contribute solutes. Moreover, milling increases the reactive surface of the sample, which may enhance mineral reactions (such as dissolution or precipitation) and also ion-exchange.

3.3 Sequential aqueous extracts

Sequential aqueous extractions involved 3–4 repeated aqueous extractions on the same sample material at a constant S/L ratio of 0.2 g/mL and extraction times of 24 h. The first sequence followed the procedure described in the previous section. At the end of the first sequence, the rock slurry that remained after filtration of the supernatant solution was again mixed with degassed, oxygen- and CO_2-free ultra-pure water, maintaining an S/L ratio of 0.2 g/mL. This procedure was repeated for another 2–3 extraction sequences.

3.4 Cation-Exchange-Capacity (CEC)

Extraction experiments for determining the CEC, i.e. the exchangeable cations adsorbed on the clay mineral surfaces, were performed on the original sample material, as well as on sequentially H_2O extracted material (section 3.3) using a constant S/L ratio of 0.2 g/mL and extraction times of 24 h. The experiments followed the same procedures as described for aqueous extracts, however, using a different extract solution. CEC measurements rely on the use of a strongly sorbing index cation that replaces all other, originally adsorbed cations. The experiments were performed at the University of Bern by using the nickel ethylenediamine (Ni-en) method elaborated by Baeyens & Bradbury (1994) and Bradbury & Baeyens (1998). The CEC is then determined from the difference between the concentrations of the index cation in the initial stock solution and in the final extract solution. Alternatively, it can be determined from the sum of the exchanged cations by measuring their concentrations in the final extract solution. For the latter method the extracted cation data need to be corrected for cations dissolved in the porewater and the cations released from (potential) mineral dissolution. Such corrections were applied based on the assumption that the main cations Na, K, Ca and Mg are attributed to the main anions Cl and SO_4 (Bradbury & Baeyens 1998, Hadi et al. 2019). The CEC is then calculated from the sum of the cations minus the concentrations of Cl and SO_4 (normalised to meq/$kg_{dry\ rock}$).

3.5 Acid extractions

Acid extractions (in combination with aqueous extractions) were performed for one sample from the BUL1-1 borehole (BUL1-1-909.24-RP; containing 4.5 wt.% calcite) using two different S/L ratios: 1) 0.05 g/mL and 2) 0.2 kg/L. Extraction time was 24 h. Degassed oxygen- and CO_2-free acetic acid (20%; 3.5 mol/L) was used for the experiments as it constitutes a weak acid that is known to dissolve carbonate but not pyrite. The acidic solution

was further diluted with ultra-pure water according to the amount of carbonate present in the sample material, thus, preventing unnecessary high acid dosing that potentially triggers unwanted mineral reactions. Final acid concentrations were 0.09 mol/L for the experiment with an S/L ratio of 0.05 g/mL and 0.35 mol/L for the experiment with an S/L ratio of 0.2 g/mL.

3.6 Chemical analyses of extract solutions

3.6.1 Measurements at the University of Bern

The chemical analyses of the extract solutions involved determination of pH, alkalinity, concentrations of the major anions and cations and for the BUL1-1 samples also dissolved organic and inorganic carbon. The alkalinity and pH were determined by using a Metrohm Titrator system (HCl titration) and Merck 4, 7 and 9 buffers. Concentrations of major cations and anions were determined at the University of Bern by ion chromatography using a Metrohm 850 ProfIC AnCat MCS IC system with automated 4–50 µl injection loops. Cation concentrations of Al, Sr, Ba, Fe and Si that either cannot be analysed by the ion chromatographic method or that were usually close to or below the detection limit, were re-analysed using a Varian 720-ES ICP-OES system. Dissolved organic and inorganic carbon was measured by infrared spectrometric techniques using an Analytic Jena Multi N/C 2100S equipped with an infrared NDIR-detector.

3.6.2 Measurements at BRGM

The measurement of pH in batch solutions was carried out with a Mettler Toledo, SevenMulti pH meter using NIST 4, 7, and 10 buffers. Alkalinity was measured using a Titrando 905 and a Dosino 800 equipped with a 5 mL syringe (Metrohm) for HCl (10^{-3} mol/L) injection. Inductively coupled plasma atomic emission spectroscopy (ICP-AES, Jobin Yvon) or mass spectroscopy (ICP-MS, Thermo Fisher Scientific) were used to measure cations concentrations. Anions were analysed by ionic chromatography (HPLC, Dionex). The elemental concentrations in solution were determined with a relative uncertainty of 3%.

3.7 Recalculating ion concentrations in extract solutions to in-situ conditions

As outlined in the introduction, conversion of solute concentrations measured in aqueous extracts to porewater solute concentrations is applicable for ions that are not involved in any

298 reactions during extraction experiments - i.e., that behave conservatively - and for which the
299 only source is the porewater. However, for clay-rich rocks, such a conversion requires that the
300 anion accessible porosity fraction is known, which is anion-specific. Anion-accessibility or
301 anion-exclusion is due to the repulsion of anions by the negatively charged surface of clay-
302 minerals, resulting in the exclusion of anions from a certain fraction of the pore space. For the
303 conservative chloride the anion-accessible porosity fraction is fairly well known (Zwahlen et
304 al., 2023; and references therein), however, not for sulphate. From double layer theory, the
305 exclusion of SO_4 in clayrocks is predicted to be higher because of its higher charge (Gimmi &
306 Alt-Epping 2018). On the other hand, SO_4 has a larger tendency to form weak complexes,
307 such as with alkaline earths, thus partly compensating the charge effect. Also, data for
308 selenate (which displays similar chemical properties as sulphate) in Opalinus Clay from Mont
309 Terri suggest a similar diffusion regime as for Cl (Gimmi et al., 2014). Thus, for the
310 experiments performed in this study a similar anion-accessible porosity fraction is used for
311 SO_4 as for Cl, which is 0.54 for Mont Terri samples (Pearson et al., 2003) and 0.52 for
312 Bülach1-1 samples (Mazurek et al., 2021). Scaling extract concentrations to in situ porewater
313 concentrations can be done via equation 1 below:

314 $$C_{free\ pw} = \frac{C_{aqex}}{(S/L) \cdot w_w \cdot f_a} \quad (1)$$

315 where $C_{\text{free pw}}$ is the in-situ solute concentration in the free porewater (mg/$L_{\text{free pw}}$), C_{aqex} is the
316 solute concentration in the aqueous extract (mg/L), S/L is the solid/liquid ratio (S = mass of
317 dry rock in grams; L = mass of ultra-pure water plus mass of porewater in millilitres), w_w is
318 the gravimetric water content (wt.%) relative to dry mass of the sample material and f_a is the
319 anion-accessible porosity fraction. Cation concentrations are reported as mg/$L_{\text{bulk pw}}$, i.e. full
320 accessibility of the pore space is assumed.
321
322 3.8 Sulphur and oxygen isotopes of dissolved sulphate in aqueous extracts

323 Analyses of $\delta^{34}S$ and $\delta^{18}O$ of dissolved sulphate in aqueous extracts were performed by
324 Hydroisotop GmbH, Schweitenkirchen, Germany. The dissolved SO_4 in the aqueous extracts
325 was precipitated as $BaSO_4$, filtered, dried and measured by Element Analyser Isotope Ratio
326 Mass Spectrometry (EA-IRMS) with an uncertainty of 0.5‰ (1σ) for both $\delta^{18}O$ and $\delta^{34}S$. The
327 measurements were normalized to the international VSMOW-scale for oxygen isotopes and to
328 the VCDT-scale for sulphur isotopes.

329

330 3.9 Geochemical modelling

331 The scope of this modelling exercise was to evaluate SO_4 data obtained from aqueous
332 extraction in terms of their compatibility with exchangeable cation data and, in more general
333 terms, with regard to their representativeness for in-situ conditions based on the well-
334 established database of the Mont Terri Rock Laboratory (Wersin et al., 2022). For this
335 purpose, a hypothetical exchanger composition was calculated from aqueous extraction data
336 (S/L ratios of 1 g/mL) based on simple geochemical modelling and then compared with the
337 exchanger composition obtained from Ni-en extracts on the same samples. The calculations
338 were performed for the Opalinus Clay samples from the Mont Terri Rock Laboratory. The
339 modelling approach relies on some simplifying assumptions, including:

340 • The ionic charge is assumed to be carried by the main compounds Na, Ca, Mg, Cl and
341 SO_4. Other compounds, such as TIC, K and Sr were neglected.
342 • The Ca concentrations of in-situ porewater were derived from assuming gypsum
343 equilibrium. Note that this reflects the maximum possible Ca concentration. Mg
344 concentrations were set to the same concentrations as Ca (based on the similarity of
345 their concentrations in OPA porewater at the Mont Terri Rock Laboratory; Wersin et
346 al., 2022).
347 • Na concentrations of in-situ porewater are derived via charge balance.

348 The calculations were performed using PHREEQC (Parkhurst & Appelo, 2013) and the
349 PSI/Nagra 2012 thermodynamic database (Thoenen et al., 2014) assuming a temperature of
350 25°C. In a first step, Cl and SO_4 concentrations from the aqueous extracts were recalculated to
351 in-situ conditions (section 3.7), then Na-Ca-Mg-Cl-SO_4 solutions were speciated, assuming
352 gypsum equilibrium and charge balance as mentioned above. In a next step, the corresponding
353 exchanger compositions were derived considering cation exchange selectivity coefficients for
354 Opalinus Clay from Pearson et al. (2011) and the cation exchange capacities obtained from Ni
355 consumption of the corresponding Ni-en extracts. The calculated exchanger compositions
356 were then compared with those obtained from Ni-en extracts.

357

358 **4 Results and discussion**

359 4.1 Bulk-rock mineralogy, carbon, total sulphur and gravimetric water content

360 Table 1 shows the mineralogy of the investigated samples based on XRD and CNS analyses,
361 as well as water contents based on gravimetry. All samples show clay-mineral, carbonate and

quartz contents in the range of 28 – 72 wt.%, 7 – 26 wt.% and 12 – 35 wt.%, respectively. Based on the classification of Füchtbauer (1988) and Naef et al. (2019) they are all classified as very sandy/silty claystones. Pyrite contents range from <1 to 2 wt.% but sulphate minerals were detected by XRD (sensitivity of approx. 1 wt.%). Organic carbon ranges from 0.4 wt.% to 1.1 wt.%.

Tab. 1: Results of bulk-rock mineralogical analyses by XRD and CNS, as well as gravimetric water contents of the investigated samples.

[wt.%]	BCI-21-550-600	BCI-21A-296-319	BCS-7	BUL1-1-858.60-RP	BUL1-1-909.24-RP	BPF1-4.30m	BPF1-3.90m
Calcite	5.6	No XRD and CNS data available	11.4	25.9	4.5	17.23	19.4
Dolomite / Ankerite	<1		<1				
Albite	1.7		1.2	3.6	3.4	1.8	2.7
K feldspar	2.9		2.3	5.6	5.7	2.6	2.7
Pyrite	2.0		1.1	1.3	<1	<1	1.8
Siderite	1.2		2.5		2.5		2.1
Quartz	15.0		13.4	34.6	21.8	12.3	11.8
Anhydrite							
Celestite							
Clay minerals	71.5		67.4	28.6	61.4	66.0	60.1
S	1.09		0.58	0.68	0.39	0.63	0.94
C(inorg)	0.83		1.74	3.11	0.81	2.07	2.57
C(org)	1.07		0.84	0.43	1.01	0.75	0.80
Water content relative to wet weight	7.37	7.11	7.31	3.77	4.81	6.93	6.51
Water content relative to dry weight	7.96	7.65	7.89	3.92	5.01	7.45	6.96

4.2 Aqueous extracts at different S/L ratios, extraction times, sample masses and sample preparation

Figure 3 shows the results of aqueous extracts performed on Mont Terri samples at different S/L ratios and at constant extraction time of 24 h using crushed and milled sample material. At S/L ratios ≤0.2 g/mL chloride concentrations in the aqueous extracts slightly increase with increasing S/L ratio to values of around 10.8 – 11.9 g/$L_{free\ pw}$ and remain at constant levels towards higher S/L ratios suggesting conservative behaviour (similarly, conservative behaviour is suggested for bromide; not shown in Fig. 3). There is a good agreement with the chloride concentrations from squeezed waters and borehole waters (Fig. 3a; Mazurek et al.,

2017; Waber & Rufer 2017; Wersin et al., 2020). Sulphate concentrations vary between 5.2 and 7.3 g/$L_{free\ pw}$ but individual samples show constant concentrations as a function of S/L ratio. However, these concentrations are by a factor of around 3–4 higher than those obtained from squeezed and borehole waters (Fig. 3b). Note that this difference cannot simply be attributed to anion-accessibility, which is somewhat uncertain for sulphate (section 3.7), it is also observed – to a lesser degree (by a factor of around 1.5–2) – when scaling SO_4 concentrations to water-loss porosity (i.e. bulk porewater concentrations when assuming f_{SO4} = 1).

Strontium and calcium concentrations show very similar and distinct trends as a function of S/L ratio, clearly indicating non-conservative behaviour, likely attributed to calcite dissolution (see below). Moreover, at S/L ratios ≤0.2 g/mL there are large differences in ion concentrations depending on whether crushed or milled sample material was used for the experiments. Extracts of the latter systematically show higher ion concentrations. These differences decrease with increasing S/L ratio. The exact reason(s) for this behaviour is not known, however, it is conceivable that milling potentially induces unwanted effects such as an increase of the reactive surface of the sample material which enhances mineral reactions, evaporation of porewater and milling induced opening of fluid inclusions potentially present in mineral phases (mainly in quartz and carbonates). In any case, the inventory of dissolved strontium (0.8–8.4 mg/$L_{bulk\ pw}$) in aqueous extracts is far too low to explain the "excess sulphate" (4–6 g/$L_{free\ pw}$) by celestite dissolution alone. The only possibility how celestite dissolution could explain the "excess sulphate" would be adsorption of the released strontium by the clay minerals owing to a shift in the cation exchange equilibrium. This is further discussed in section 4.4. Barium concentrations (not shown in Fig. 3) show a similar trend as observed for Sr, however, at distinctly lower concentrations (<1 mg/$L_{bulk\ pw}$).

The pH (Fig. 3e) continuously decreases as a function of S/L ratio (from around 9.3–9.8 down to 8.3–8.8). This trend mainly reflects the higher buffer capacity of extracts performed at high S/L ratios, which results from the comparatively higher content of clay minerals (i.e., the larger surface area available for complexation reactions; see Wersin & Pękala 2017, Wersin et al., 2020).

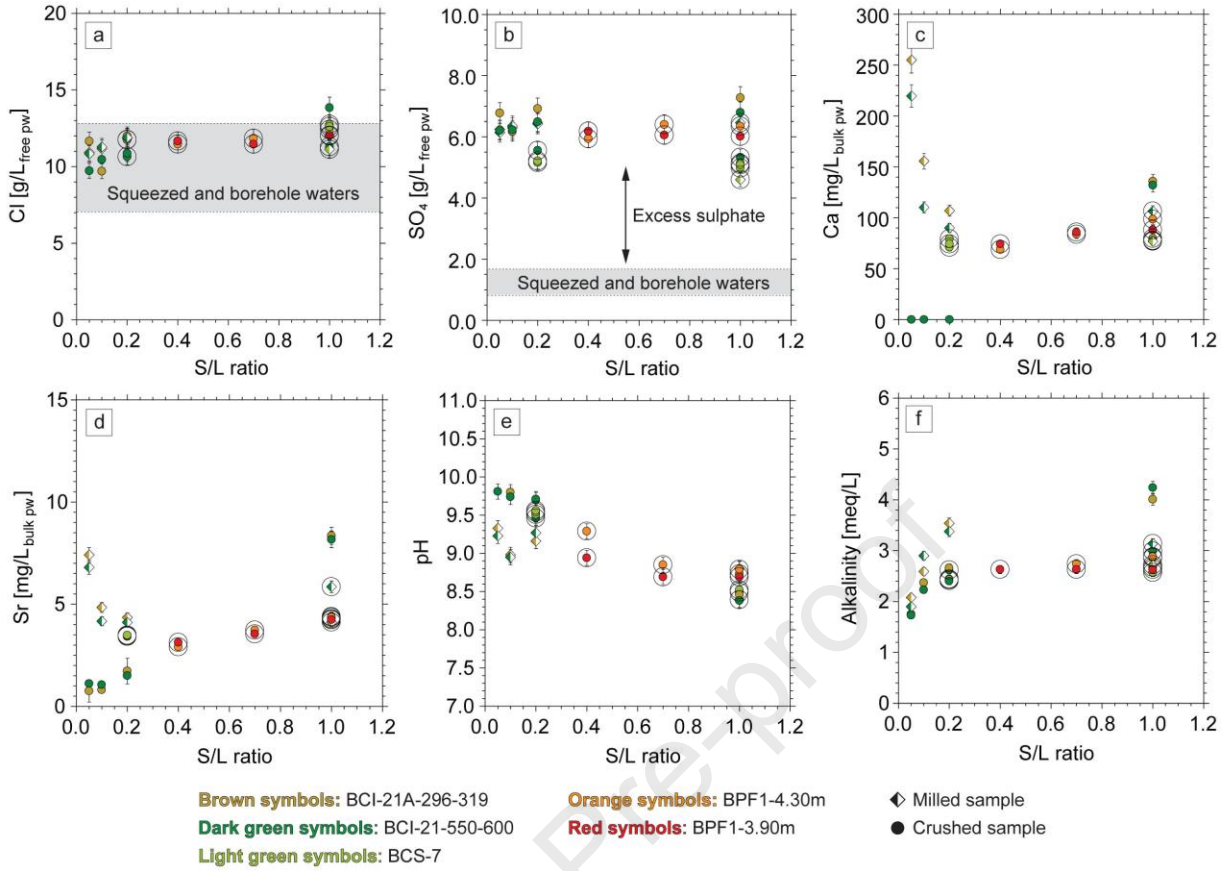

Fig. 3: Results of aqueous extracts performed on Mont Terri samples at variable S/L ratios. Extraction time was 24 h. Experiments with black circles were performed at the University of Bern. Calcium concentrations plotting at zero are below the detection limit of 0.5 mg/$L_{extract}$. Data for squeezed and borehole waters are from Mazurek et al. (2017) and Pearson et al. (2003). Concentrations of Cl and SO_4 are recalculated to in-situ conditions using an anion-accessible porosity fraction of 0.54 (Person et al., 2003).

Alkalinity shows an increase at low S/L ratios (≤0.2 g/mL) and virtually constant values at higher S/L ratios (Fig. 3f). A similar trend is observed for the calculated calcite saturation indices of the aqueous extracts at variable S/L ratios (i.e. for original extract concentrations; Fig. 4a). For the calculation of saturation indices the software PHREEQC by Parkhurst & Appelo (2013) and the PSI/Nagra 2012 thermodynamic data base (Thoenen et al., 2014) were used. Fort S/L ratios >0.2 g/mL calcite dissolution during aqueous extraction imposed equilibrium or-near-equilibrium conditions, whereas undersaturation with respect to calcite is observed for aqueous extracts with S/L ratios ≤0.2 g/mL, probably owing to a limitation in the availability of calcite at these low S/L ratios.

Saturation indices for strontianite show a similar trend as for calcite, however, the extracts being slightly undersaturated even at S/L ratios >0.2 g/mL (Fig. 4b). The calculated partial pressure of CO_2 generally increases with increasing S/L ratio from around 10^{-5}–10^{-4} bar to 10^{-}

$^{3.5}$ bar (Fig. 4c) and with distinct differences between extracts of crushed and milled material for low S/L ratios. Note that the sub-atmospheric pCO_2 levels result from using degassed water as extract solution and the CO_2-free atmosphere of the glovebox in which the experiments were performed (section 3.2). The saturation indices of celestite and gypsum continuously increase with increasing S/L ratio but remaining distinctly undersaturated (Fig. 4d,e).

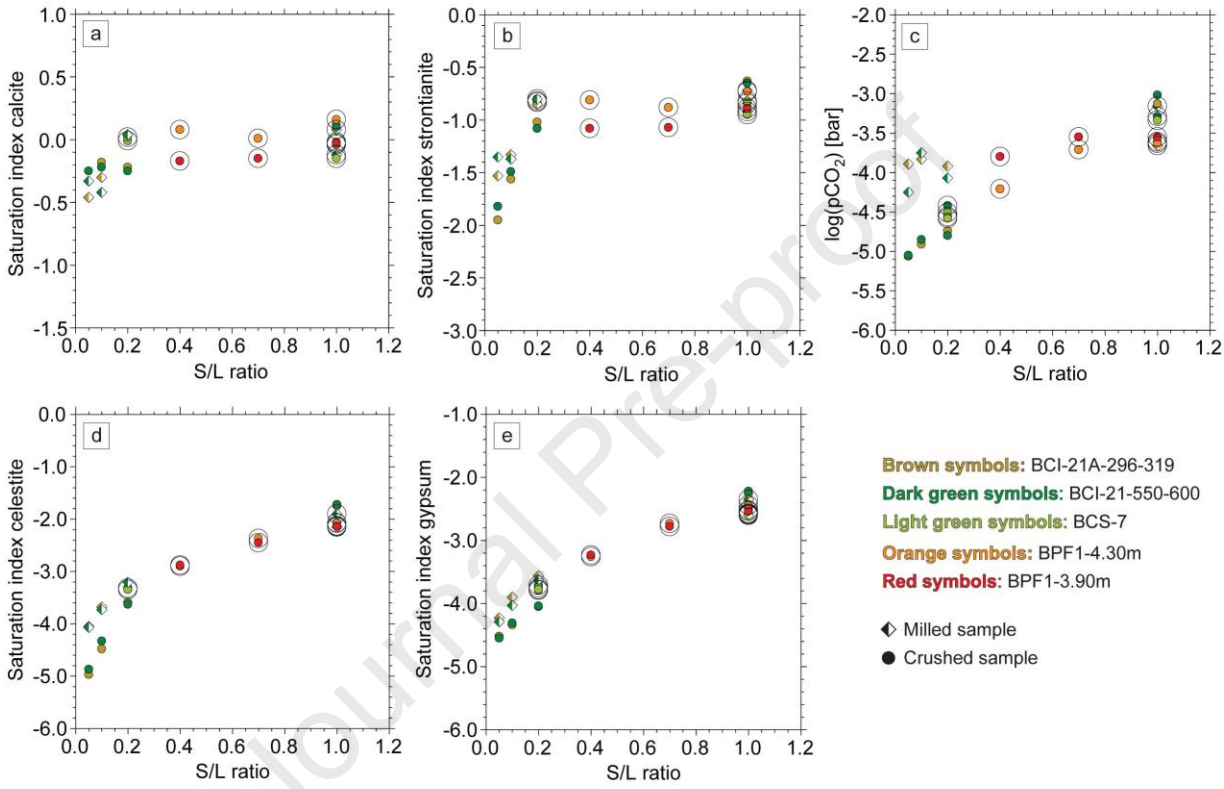

Fig. 4: Calculated mineral saturation indices of aqueous extracts (i.e. for original extract concentrations) performed on Mont Terri samples at variable S/L ratios. For the modelling the software PhreeqC and the PSI/Nagra 2012 data base (Thoenen et al., 2014) were used. Experiments with black circles were performed at the University of Bern.

In addition to extraction experiments at variable S/L ratios and constant extraction time and sample mass, kinetic tests were performed at constant S/L ratios but variable extraction times (10 min up to 7 days) and sample masses (4–20 g). Sulphate and chloride concentrations ($mg/L_{bulk\ pw}$), as well as pH and alkalinity are virtually constant as a function of these experimental parameters. Note that the constant SO_4 concentrations as a function of extraction time and S/L ratio, as well as the lack of correlation between "excess sulphate" and pyrite content of the samples (see Tab. 1) indicate that oxidation reactions are deemed to have been successfully supressed during aqueous extraction.

4.3 Sequential aqueous extracts

Figure 5 shows the concentrations of chloride and sulphate, as well as their ratios for sequential aqueous extracts of Mont Terri samples. All of the investigated samples show the same general trends with strongly decreasing concentrations upon progressively diluting the porewater until complete removal after the third extraction sequence (Figs. 5a,b). Contrastingly, the SO_4/Cl ratio exponentially increases (Fig. 5c) suggesting release from a sulphate-bearing phase. Accordingly, no fully conservative behaviour can be attested for sulphate. However, from a quantitative perspective, the SO_4 released during the second, third and fourth extraction sequence is only of minor importance. If the same behaviour is assumed for sulphate as for chloride – a conservative species – then the absolute increase of sulphate in the subsequent extractions is in the range of 44–292 mg/$L_{free\ pw}$, thus only a small amount compared to the amount leached during the first extraction step (Fig. 3b). Consequently, the source of the "excess sulphate" constitutes a limited reservoir that is almost completely exhausted during the first extraction.

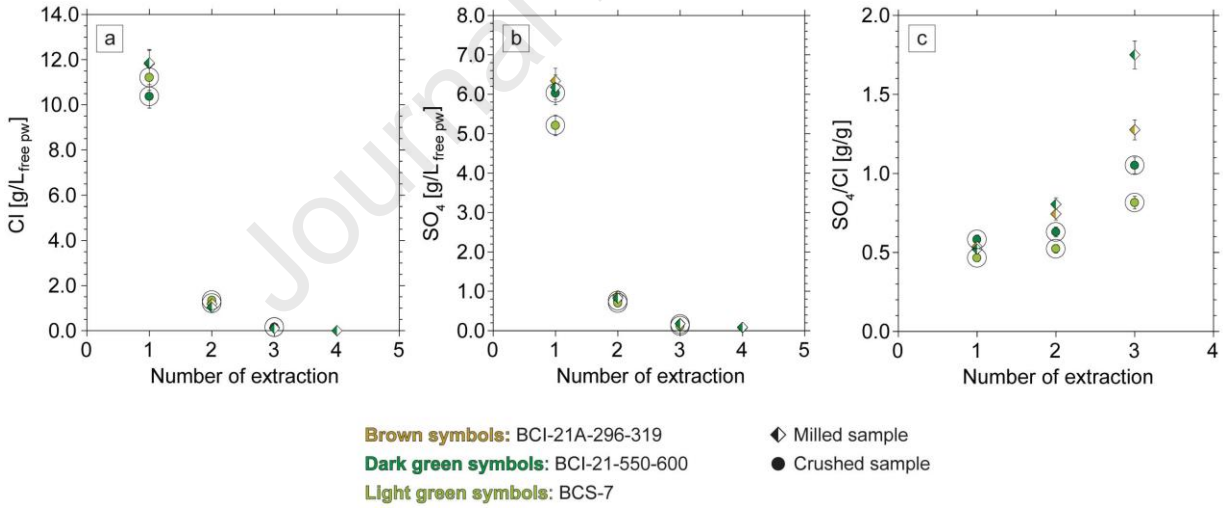

Fig. 5: Concentrations of Cl and SO_4 (recalculated to in-situ conditions using an anion-accessible porosity fraction of 0.54; Person et al., 2003) and their ratios during sequential aqueous extraction of Mont Terri samples. Experiments with black circles were performed at the University of Bern.

4.4 Ni-en extracts

Figure 6 illustrates the results of the Ni-en extractions of Mont Terri samples. The CEC derived from Ni consumption ranges from 89.8 to 116.0 meq/kg_{rock} for sample BCS-7 and 104.0–134.7 meq/kg_{rock} for sample BCI-21-550-600 (Fig. 6a). The values for the CEC derived

476 from the corrected sum of cations agree reasonably well. The small differences in Ni
477 consumption and sum of cations between the two investigated samples reflect the
478 comparatively higher clay mineral content of sample BCI-21-550-600 sample (Tab. 1). Both
479 of the investigated samples show the same general trends with slightly lower CEC derived
480 from Ni-en extracts of original sample material compared to the CEC derived from Ni-en
481 extracts of previously H_2O extracted material. For extracts of the original sample material the
482 main extracted cation is Na, followed by Ca and Mg (Fig. 6b–d). During progressive dilution
483 of the porewater (i.e. with increasing number of sequential H_2O extractions), Ca and Na
484 concentrations show opposed trends in the Ni-en extracts with increasing Ca concentrations
485 and equally decreasing Na concentrations. This is because the total solute concentration
486 affects the selectivity of the exchanger for Ca in that the higher charged ion is preferred more
487 strongly on the exchange sites when the total solute concentration in the solution decreases
488 (Gaines & Thomas 1953). Accordingly, the trends observed for Ca in aqueous extracts as a
489 function of S/L ratio (i.e. different degrees of dilution of the porewater; Fig. 3c) do not only
490 reflect calcite dissolution (section 4.2) but also variable magnitudes of cation exchange.
491 Magnesium on the other hand appears much less sensitive to such an effect (Fig. 6d),
492 potentially reflecting differences in the dissolution kinetics between calcite and dolomite.
493 Strontium concentrations in Ni-en extracts are low, ranging from 0.85 to 1.31 meq/kg_{rock}
494 corresponding to 0.008–0.010 equivalent fractions on the clay exchanger (Fig. 6e). Modelling
495 of seepage waters at Mont Terri indicates SrX_2 equivalent fractions that are a factor 2–3 lower
496 than those obtained from Ni-en extracts. This difference has been explained by the dissolution
497 of celestite during Ni-en extraction (Wersin et al. 2020). Since the exchangeable strontium in
498 the Ni-en extracts of the sequentially H_2O extracted material does not markedly vary (Fig.
499 6e), dissolution of the Sr bearing mineral phase must have occurred mainly during the first
500 sequence of aqueous extraction, which is in line with the results from sequential aqueous
501 extracts (section 4.3). However, the strontium inventory (dissolved plus exchanged) is not
502 sufficiently large to explain the "excess sulphate" by celestite dissolution alone (~0.8 g/$L_{free\ pw}$;
503 Fig. 6f). Thus, celestite constitutes a limited SO_4 reservoir that is completely exhausted in
504 each extraction. Barium concentrations are below the detection limit of 0.05 mg/$L_{extract}$
505 (corresponding to 0.004 meq/kg_{rock} or 3.4 mg/$L_{bulk\ pw}$) in all analysed extracts.
506

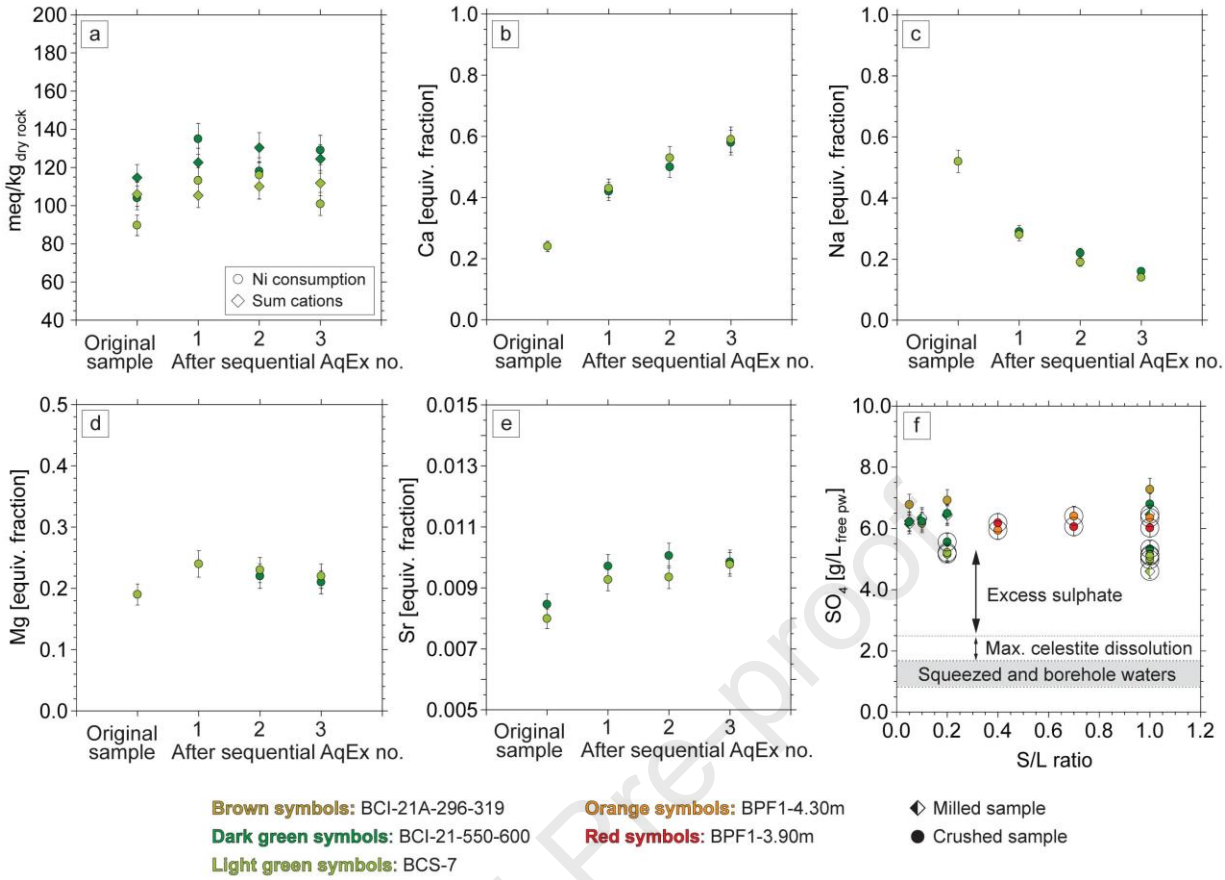

Fig. 6: a–e) Results of Ni-en extractions of Mont Terri samples. The extraction tests were performed on the original sample material, as well as on sequentially H_2O extracted material. f) Inventory of strontium (dissolved plus exchanged) is not sufficiently large to explain the "excess sulphate" in aqueous extracts by celestite dissolution alone. Data for squeezed and borehole waters are from Mazurek et al. (2017) and Pearson et al. (2003). Concentrations of Cl and SO_4 are recalculated to in-situ conditions using an anion-accessible porosity fraction of 0.54 (Person et al., 2003).

4.5 Acid extracts

Acid and aqueous extracts were performed on a drillcore sample from the Bülach1-1 borehole and the results are illustrated in Fig. 7. Chloride concentrations in aqueous extracts (11.9–13.1 $g/L_{free\ pw}$) agree well with those in squeezed and advectively displaced waters. At low S/L ratios (0.05 g/mL) acid extracts show slightly higher Cl concentrations compared to aqueous extracts. This difference becomes distinctly larger at higher S/L ratios (0.2 g/mL). Moreover, at higher S/L ratios the acid extract of milled material shows much larger Cl concentrations compared to the acid extract of crushed material. For chloride, which has shown to be a conservative anion (section 4.2; Wersin et al., 2020 and references therein), these differences are likely to reflect contributions from fluid inclusions. As fluid inclusions are not homogeneously distributed within the rock – in OPA they are potentially associated with diagenetic calcite and detrital quartz – the intensity of this effect can vary among extracts of

the same sample. However, in general it can be assumed that the contribution of fluid inclusions increases with 1) increasing S/L ratio, 2) with increasing calcite and/or quartz contents and 3) with increasing mineral dissolution (e.g. favoured by increasing the reactive surface of a sample by milling).

Similar differences between aqueous and acid extractions are also observed for sulphate, however, somewhat less well pronounced. Moreover, sulphate concentrations derived from extracts of crushed and milled material show good agreement. The same applies to the Mont Terri samples, SO_4 concentrations in aqueous extracts are a factor of 3–4 higher compared to those obtained from direct porewater sampling techniques. For obvious reasons Ca concentrations are much higher in acid extracts than in aqueous extracts (Fig. 7c). By taking this difference as a rough measure for how much calcite is dissolved during acid extraction, a value of around 90% is obtained. Acid extracts at an S/L ratio of 0.2 g/mL show SO_4 concentrations that are about 1.6 mg/$L_{free\ pw}$ higher than in aqueous extracts (Fig. 7b). If we assume that the difference is exclusively due to dissolution of calcite containing SO_4 impurities, and that calcite dissolution that potentially occurs during aqueous extraction is insignificant compared to that occurring during acid extraction, then the calcite must contain around 700 – 800 ppm sulphate. At first sight this value appears rather high, however, Wynn et al. (2018) have shown that calcite that precipitates under lab conditions from low-ionic strength solutions of pH 7–8 and containing 2 mg/L SO_4, incorporates around 100 ppm sulphate. Moreover, they show that keeping the pH constant but increasing the sulphate concentration of the parent solution to 20 mg/l increases the amount of the incorporated sulphate to 400 – 450 ppm. Considering that a substantial part of the carbonate in the Opalinus Clay is biogenic and, thus, precipitated from seawater with around 2.7 g/L sulphate, then 700 – 800 ppm sulphate incorporated in calcite is not unrealistic. This is corroborated by Lerouge et al. (2014) who found sulphur contents of <500 ppm and <2000 ppm in diagenetic calcite and bioclastic material, respectively, in the Opalinus Clay of the Benken borehole in northern Switzerland. Nevertheless, the acid extractions show that the sulphate concentrations in calcite – although they appear to be rather high at first sight – are far too low to explain the "excess sulphate" in the aqueous extracts by congruent calcite dissolution. For example, taking the calcium inventory (dissolved plus exchanged) as a rough measure of the maximum amount of calcite that was dissolved during aqueous extraction, then a value of around 4% is obtained. Dissolution of 4% of the available calcite contributes roughly 60 mg/$L_{free\ pw}$ sulphate, thus a very small amount compared to the "excess sulphate" (Fig. 7b). Moreover, it must be recalled that the concentration of 700 – 800 ppm sulphate in calcite was determined

based on the assumption that all of the sulphate in the acid extracts originates from calcite dissolution and thus, the 700 – 800 ppm represent a maximum value.

Strontium and barium show detectable concentrations only in the acid extracts. Also iron is present in the acid extracts at rather high concentrations (0.3 – 1.0 g/$L_{extract}$ depending on S/L ratio; not shown in Fig. 7). Potentially this iron could originate from pyrite dissolution. However, taking into account that acid extracts performed at S/L ratios of 0.05 g/mL show similar sulphate concentrations as the aqueous extracts, pyrite dissolution is not considered to play a major role. Most likely the iron stems from the dissolution of Fe-bearing carbonates: based on the XRD data (Tab. 1) the investigated Bülach1-1 sample contains 2.5 wt.-% siderite and thus, providing sufficient iron to explain the observed concentrations.

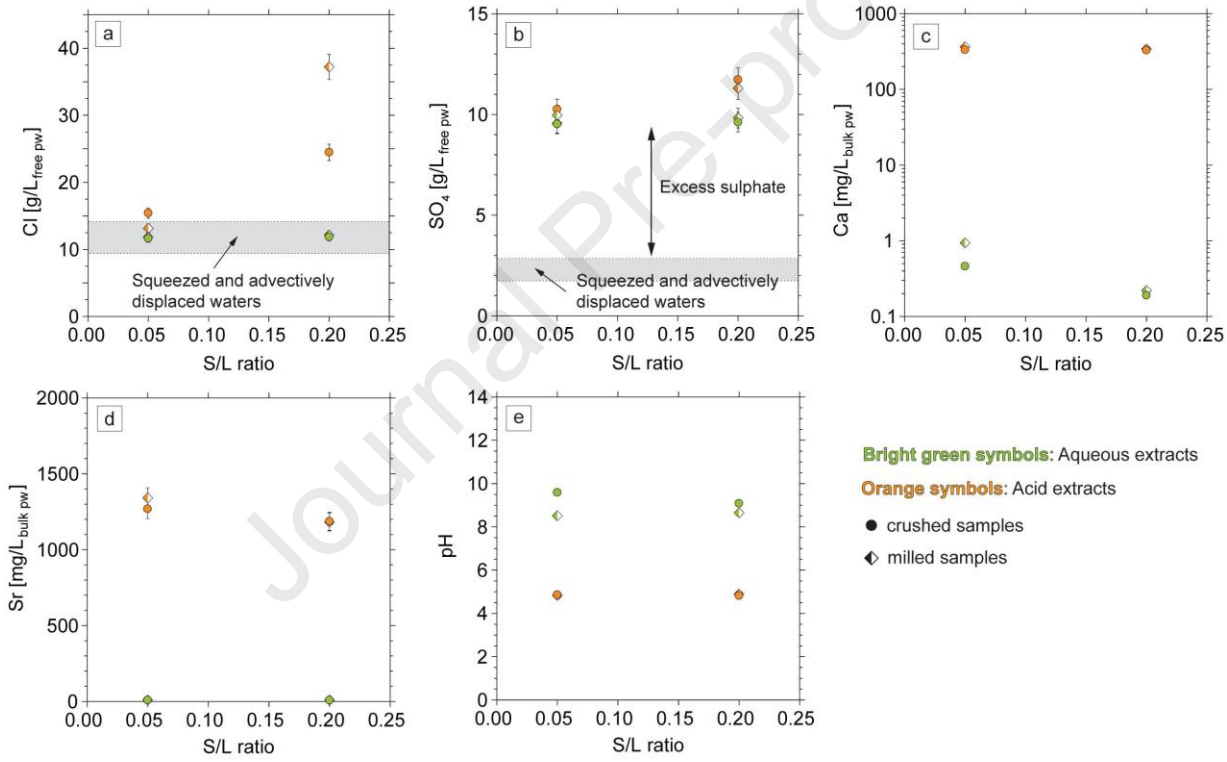

Fig. 7: Results of acid and aqueous extracts of the Bülach1-1 sample. All experiments performed at University of Bern. Data for squeezed and advectively displaced waters are from Mazurek et al. (2021) Concentrations of Cl and SO_4 are recalculated to in-situ conditions using an anion-accessible porosity fraction of 0.52 (Mazurek et al., 2021).

4.6 Dissolved organic carbon in aqueous extracts

Figure 8 shows DOC concentrations in aqueous extracts of the Bülach1-1 samples as a function of S/L ratio, sample preparation and sulphate concentration. For comparison data from squeezed and advectively displaced waters are illustrated too (Mazurek et al., 2021).

582 Note that DOC concentrations in aqueous extracts are reported as mg/$L_{bulk\ pw}$. However, a
583 significant part of the dissolved organic material (DOM) contains anionic functional groups
584 (Huclier-Markai et al., 2010; 2018) and, thus, the DOM likely behaves similar as inorganic
585 anionic compounds, i.e., it is affected by anion exclusion and no or only weak sorption
586 (Charlet et al. 2017, Chen et al. 2018). Consequently, DOC concentrations in the free
587 porewater are somewhat higher compared to the concentrations in the bulk porewater
588 illustrated in Fig. 8. For the investigated samples the DOC concentrations in aqueous extracts
589 vary as a function of sample preparation – i.e. extracts of milled material consistently show
590 higher concentrations than extracts of crushed material – and also as a function of S/L ratio –
591 i.e. extracts performed at low S/L ratios show higher concentrations than extracts performed
592 at high S/L ratios. In contrast, sulphate concentrations do not markedly vary neither as a
593 function of sample preparation nor as a function of S/L ratio (Fig. 8). Overall, this lack of
594 correlation between DOC and sulphate concentration indicates that sulphur associated with
595 organic matter is not likely to be the source of the "excess sulphate" in aqueous extracts. This
596 is supported by mass balance considerations: For example, the aqueous extract of milled
597 sample material at an S/L ratio of 0.05 g/mL, shows DOC concentrations that are ~1.5 g/$L_{bulk\ pw}$ higher than those of squeezed waters. If the difference in sulphate concentration between
599 squeezed waters and the aqueous extract is due to sulphur released from dissolved organic
600 matter, then the DOM must show C/S mass ratios of around 0.75 (or slightly higher
601 considering anion exclusion for DOM; see above). This value then decreases with decreasing
602 difference in DOC between aqueous extracts and squeezed waters. Such low C/S mass ratios
603 are not considered realistic. Thus, a major release of sulphur from dissolved organic material
604 during aqueous extraction experiments, which could explain the "excess sulphate", is
605 unlikely.
606

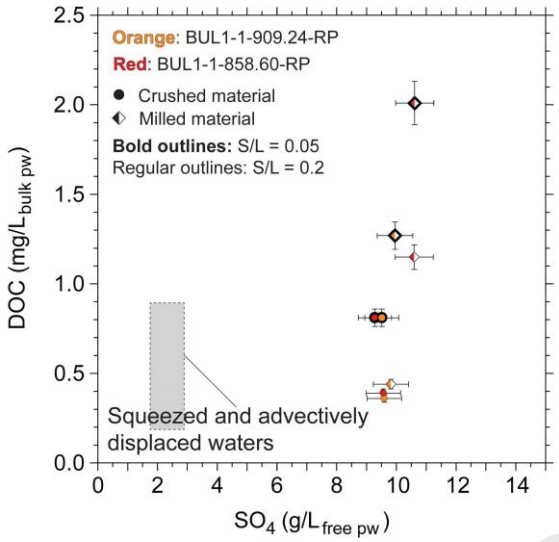

Fig. 8: Concentrations of sulphate and dissolved organic carbon (DOC) in aqueous extracts of Bülach1-1 samples. For comparison data from squeezed and advectively displaced waters are illustrated too (Mazurek et al., 2021). Sulphate concentrations are recalculated to in-situ conditions using an anion-accessible porosity fraction of 0.52 (Mazurek et al., 2021).

4.7 Sulphur and oxygen isotopes in aqueous extracts and borehole water at Mont Terri

Re-equilibration during aqueous extraction does not only affect chemical constituents but also isotopes. Thus, the oxygen and sulphur isotope composition of dissolved sulphate in aqueous extracts reflects contributions from 1) the original porewater 2) mineral reactions and 3) oxygen isotope exchange between dissolved SO_4 and H_2O. However, the latter is very slow and not relevant on timescales of the extraction experiments (Krouse & Mayer, 2000).

Figure 9a shows the $\delta^{18}O$ and $\delta^{34}S$ values of dissolved sulphate in aqueous extracts of the Mont Terri samples. For comparison it also includes isotope data for vein celestite in the Opalinus Clay at Mont Terri (Pearson et al., 2003), whole-rock gypsum and/or anhydrite from the underlying Triassic evaporites (Gipskeuper, Muschelkalk; Mazurek & de Haller, 2017), marine sulphate during different geological periods (Claypool et al., 1980 and Balderer et al., 1991) and sulphate in present-day porewater (borehole waters) of the Opalinus Clay at Mont Terri (Pearson et al., 2003; Müller and Leupin, 2012). Figure 9b shows a histogram for the $\delta^{34}S$ values of diagenetic pyrite and sphalerite from the Dogger–Liassic rock sequence at Mont Terri (De Haller et al., 2014). They show a Gaussian distribution, ranging widely from -48.2‰ VCDT to 57.8‰ VCDT, centred at 0‰ VCDT. Pyrite from the Benken borehole analysed by Lerouge et al. (2014), falls within the same range.

$\delta^{18}O$ and $\delta^{34}S$ values of dissolved sulphate in aqueous extracts range between 11.6–12.8‰ VSMOW and 23.3–25.1‰ VCDT, respectively. These values are in good agreement with the

present-day porewater in the Opalinus Clay at Mont Terri, which is enriched in ^{34}S relative to Mesozoic marine sulphate and depleted in ^{18}O relative to vein celestite (Fig. 9a). Although partly overlapping, $\delta^{34}S$ values of sulphide minerals in the OPA are generally lower than those of dissolved sulphate in aqueous extracts. Thus, the isotope composition of dissolved sulphate in aqueous extracts seemingly represents the original porewater in the Opalinus Clay without any major contributions from e.g. sulphide mineral oxidation or celestite dissolution. As a hypothesis, the "excess sulphate" could be weakly bound to mineral surfaces, so that isotopes can readily exchange with the porewater. In fact, laboratory and field experiments have shown that sulphur and oxygen isotope fractionation during adsorption and desorption of sulphate is negligible (Mayer et at., 1995; Van Stempvoort et at., 1990). In contrast, sulphate that is strongly bound in crystal lattices of e.g. celestite is fractionated relative to porewater sulphate (Fig. 9) and a shift away from the porewater isotope signature would be observed if congruent mineral dissolution is the main contributor for the "excess sulphate" in aqueous extracts. However, this is not the case.

Sorption of sulphate is well known for soils, where pH (Guadalix & Pardo 1991, Bhatti et al. 1997) and the presence of hydrous oxides of iron and aluminium (Chao et al. 1964a, Fuller et al. 1985) are the main controlling factors but also total sulphate concentrations, ionic strength, competing anions and clay content can have an influence (Chao et al. 1964b, Charlet et al. 1993, Comfort et al. 1992, Inskeep 1989). For indurated claystones, such as the Opalinus Clay, anionic sorption has been much less studied and very little is known regarding the uptake mechanisms. Also, there are some reservations concerning its relevance at high pH conditions. Anionic sorption mainly operates at low pH (i.e., below the point of zero charge of clay-minerals), whereas at high pH it is considered small to negligible (e.g. Guadalix & Pardo 1991). However, in batch, column and through-diffusion experiments using Callovo-Oxfordian claystone samples, Bazer-Bachi et al. (2007) and Descostes et al. (2008) observed a weak retention of sulphate that depends on the mineralogical composition of the solid phase and the sulphate concentration in the porewater with K_d values of 0.15–0.37 L/kg for sulphate concentrations in the range of 5×10^{-7} to 4.4×10^{-3} mol/L at a pH of 7.3. Similarly, Van Loon et al. (2018) also observed a weak retention of sulphate in through-diffusion experiments performed on Opalinus Clay samples. The derived K_d values of 0.06–0.09 L/kg for sulphate concentrations of 10^{-2} mol/L (pH = 7.9) are in good agreement with the findings of Bazer-Bachi et al. (2007), i.e., extrapolating their Langmuir fit. These K_d values imply concentrations of weakly bound SO_4 of 0.6–0.9 mmol/kg_{rock}. This corresponds to a contribution of roughly 1.7–2.6 g/$L_{free\ pw}$ from aqueous extracts, i.e., not large enough to

explain the "excess sulphate" (~ 35–52%). Note that although sulphate retention has been demonstrated for indurated claystones, the exact mechanism could not be identified in the aforementioned studies. One hypothesis is that kaolinite significantly contributes to the retention of sulphate in claystones as indicated by previous experimental studies (Rao & Sridharan 1984, Matusik 2014, Sadeghalvad et al. 2021). However, at the current stage it is not entirely clear why weakly bound sulphate would be released during aqueous extraction: concerning sorption processes the mixing of the water-saturated rock sample with ultra-pure water imposes a strong dilution of the porewater, i.e. the ionic strength of the system decreases and the electrostatic effect results in a anionic sorption than compared to in-situ conditions (Charlet et al. 1993). In contrast, anionic sorption is stronger at a pH of 7 (i.e., in-situ conditions) compared to a pH of around 9 (i.e., aqueous extracts; Guadalix & Pardo 1991). However, it is not considered likely that this difference in pH would make a major difference in the amount of sulphate released. Thus, currently this remains on a hypothetical level and further efforts must be taken in order to better constrain potential contributions from weakly bound sulphate.

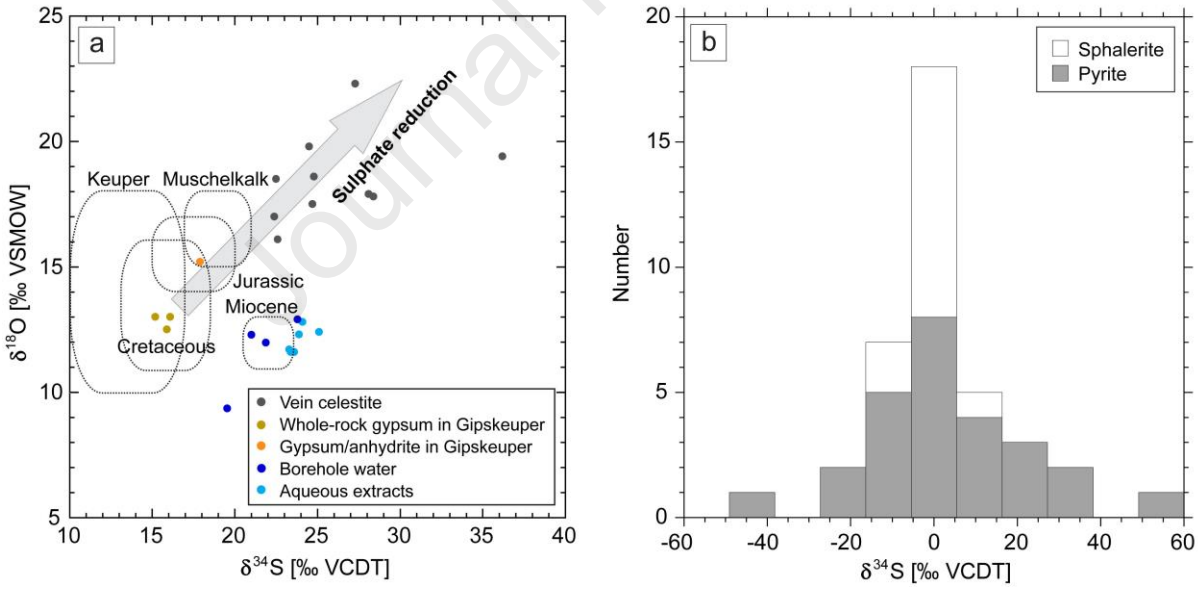

Fig. 9: $\delta^{18}O$ and $\delta^{34}S$ values for dissolved sulphate in aqueous extracts of Mont Terri samples compared to the isotopic composition of sulphate of vein celestite (Pearson et al., 2003), whole-rock gypsum and/or anhydrite from the underlying Triassic evaporites (Gipskeuper, Muschelkalk; Mazurek & de Haller, 2017), marine sulphate during different geological periods (Claypool et al., 1980 and Balderer et al., 1991) and sulphate in present-day porewater (borehole waters) of the Opalinus Clay at Mont Terri (Pearson et al., 2003; Müller and Leupin, 2012). Analytical uncertainties are 0.5‰ (1σ) for both $\delta^{18}O$ and $\delta^{34}S$. b) Histogram for the $\delta^{34}S$ values of diagenetic pyrite and sphalerite from the Dogger–Liassic rock sequence at Mont Terri (de Haller et al., 2014).

4.8 Plausibility checks by geochemical modelling

The plausibility of the SO_4 data from aqueous extracts in terms of their representativeness for in-situ conditions was tested by simple geochemical modelling as described in section 3.9. On the basis of the Cl and SO_4 concentrations recalculated to in-situ conditions, a simplified exchanger composition including the main cations Na, Ca and Mg was derived for four of the Mont Terri samples. The calculations yield high exchangeable Na occupancies of ~0.8 (equivalent fraction; Fig. 10a) and low exchangeable Ca + Mg occupancies of ~0.2 (equivalent fraction; Fig. 10b). These results are at odds with the exchanger composition obtained from Ni-en extracts of the same samples, which yield distinctly lower Na but higher Ca + Mg occupancies. The latter data are, however, in good agreement with Ni-en extraction data reported by Wersin et al. (2022) as well as with data calculated from borehole waters. This comparison indicates that SO_4 recalculated from aqueous extracts implies dissolved and exchangeable cation concentrations which are not compatible with the measured exchangeable cation data and, in more general terms, not compatible with the well-established porewater chemistry database for Mont Terri (see compilation by Wersin et al., 2022). This simple geochemical modelling exercise thus underlines that SO_4 from aqueous extraction experiments is affected by mineral-water reactions, i.e., reflecting non-conservative behaviour.

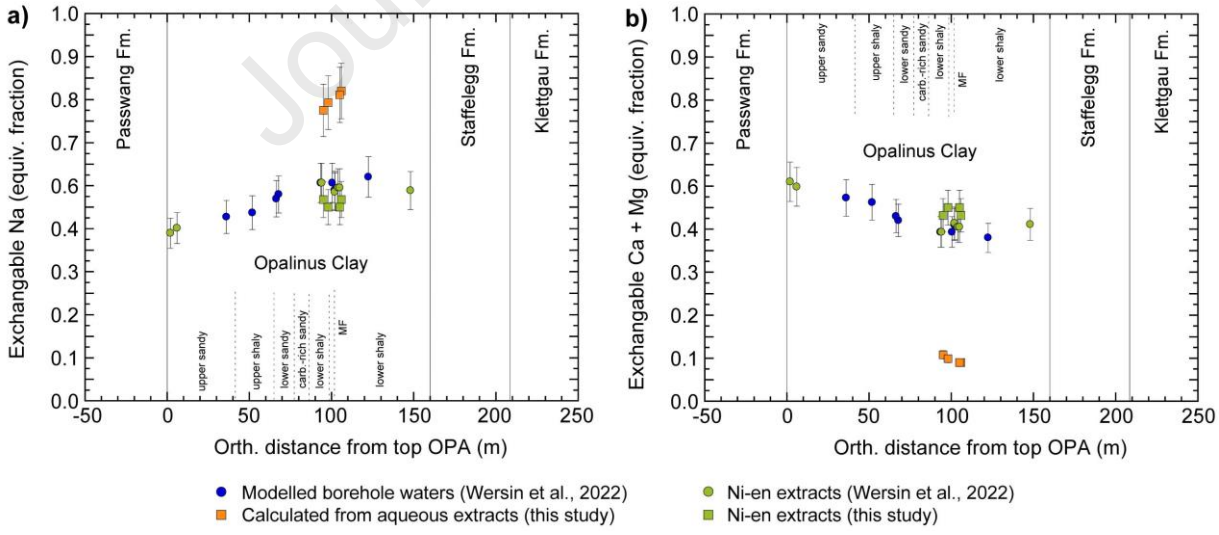

Fig. 10: a) Exchangeable Na and b) sum of exchangeable Ca+Mg (equivalent fractions) vs. distance (m) from top Opalinus Clay at the Mont Terri Rock Laboratory. Orange squares: calculated from SO_4 and Cl concentrations in aqueous extracts (see text). Green symbols: measured cation data from Ni-en extracts (corrected for dissolved cations in the porewater). Blue circles: modelled cation data based on borehole waters documented in Wersin et al. (2022).

5 Conclusions

Oxidation reactions are deemed to have been successfully supressed during aqueous extraction. This is indicated by 1) the lack of correlation between "excess sulphate" and pyrite contents in the samples, 2) constant SO_4 concentrations as a function of extraction time and S/L ratio and 3) $\delta^{18}O$ and $\delta^{34}S$ values of dissolved sulphate in aqueous extraction being in good agreement with those measured for borehole waters.

The extraction experiments yielded conservative behaviour for Cl, which is in line with earlier findings (e.g. Waber et al. 2003, Wersin et al. 2013, Waber & Rufer 2017, Wersin et al. 2020). All other cations and anions (except bromide) behave clearly non-conservatively, i.e. their concentrations in the extract solutions vary as a function of S/L ratio and extraction time. Although SO_4 concentrations in aqueous extracts are constant as a function of S/L ratio and extraction time, the SO_4/Cl ratio increases during sequential extraction indicating release from a sulphate-bearing phase, thus, suggesting non-conservative behaviour. However, from a quantitative perspective the major release occurs during the first extraction, whereas release during subsequent sequential extractions is minimal. Thus, celestite constitutes a limited SO_4 reservoir that is nearly completely exhausted in each extraction. However, Ni-en extracts show that the strontium inventory (dissolved plus exchanged) is not sufficiently large to explain the "excess sulphate" by celestite dissolution alone (roughly 15% of the "excess sulphate" can be explained by celestite dissolution). Acid extracts indicate that calcite in the Opalinus Clay contains a maximum of around 700 – 800 ppm sulphate, which is in line with a study by Wynn et al. (2018). Considering the small amount of calcite which is dissolved during aqueous extraction (~4%), these concentrations are far too low to explain the "excess sulphate" by congruent calcite dissolution. However, uncertainties exist on how the sulphur associated with calcite occurs (i.e. incorporated in the crystal lattice or as solid inclusions of an S-bearing phase) and that incongruent rather than congruent calcite dissolution could be a key process to explain the "excess sulphate" in aqueous extracts. These uncertainties could be addressed by transmission electron microscopy (TEM) and Scanning-TEM (STEM) studies, which provide high-resolution data on the quantity and spatial distribution of S in calcite.

Measurements of the dissolved organic carbon in aqueous extracts yield no correlation with sulphate concentrations. Moreover, mass balance considerations show that in order to explain the "excess sulphate", the dissolved organic material must show unrealistic low C/S mass ratios. Thus, a major release of sulphur from organic material during aqueous extraction experiments, which could explain the "excess sulphate", is unlikely.

Ultimately, the various types of extraction experiments failed to definitely identify the source of the "excess sulphate" in aqueous extracts. However, based on the good agreement between the $\delta^{18}O$ and $\delta^{34}S$ values of dissolved SO_4 in aqueous extracts and those of borehole waters the "excess sulphate" could be weakly bound to mineral surfaces (e.g. clay-minerals), so that isotopes can readily exchange with the porewater. This hypothesis is in line with diffusion studies by Bazer-Bachi et al. (2007), Descostes et al. (2009) and Van Loon et al. (2018) who observed a weak retention of sulphate in their experiments performed on Callovo-Oxfordian claystones and also Opalinus Clay samples. The retention mechanisms are not exactly known but derived K_d values imply potential sulphate contributions in the range of 1.7–2.6 $g/L_{free\ pw}$ in aqueous extracts. Together with the contributions from celestite dissolution this would explain roughly 60% of the "excess sulphate". However, there are some reservations regarding the process by which sulphate would be released during aqueous extraction. Thus, at the current state this remains on a hypothetical level and further efforts must be taken in order to better constrain potential contributions from weakly bound sulphate, e.g., by anion-exchange experiments.

Although, the reasons for the differences in SO_4 concentrations for OPA porewater derived from aqueous extraction and direct sampling techniques – i.e. borehole waters, squeezing and advective displacement experiments – are still not fully understood, the good consistency between the latter methods suggests that the derived sulphate concentrations represent the conditions in the in-situ porewater reasonably well. This is further supported by simple plausibility tests by geochemical modelling showing that SO_4 concentrations from aqueous extracts recalculated to in-situ conditions imply dissolved and exchangeable cation concentrations which are not consistent with the measured exchangeable cation data from Ni-en extracts or those calculated from borehole waters. Again, this underlines the non-conservative behaviour of sulphate during aqueous extraction.

Acknowledgements

The authors thank the Swiss National Cooperative for the Disposal of Radioactive Waste (Nagra) and the Swiss Federal Office of Topography swisstopo for generously providing drillcore samples. Moreover, we warmly acknowledge the experimental and analytical work performed by P. Bähler, C. Pichler, J. Zucha, L. Lehmann, T. Conte, C. Cosson, L. Kastler, N. Lafaurie, C. Quarton and Hydroisotop GmbH. We appreciate discussions with M. Mazurek,

H.N. Waber, U. Mäder, E. Gaucher and C. Tournassat. Ultimately, we thank Nagra for financial support.

References

Baeyens, B. & Bradbury, M.H. (1994). A Physico-Chemical Characterisation and Calculated In-situ Porewater Chemistries for a Low Permeability Palfris Marl Sample from Wellenberg. Nagra Technical Report NTB 94-22. Nagra, Wettingen, Switzerland.

Balderer, W., Pearson, F. J., & Soreau, S. (1991). Sulphur and oxygen isotopes in sulphate and sulphide. In F. J. Pearson, W. Balderer, H. H. Loosli, B. E. Lehmann, A. Matter, T. Peters, H. Schmassmann & A. Gautschi (Eds.), *Applied isotope hydrology: A case study in northern Switzerland* (pp. 227–242). Studies in Environmental Science, vol. 43. Amsterdam: Elsevier.

Bazer-Bachi, F., Descostes, M., Tevissen, E., Meier, P., Grenut, B., Simonnot, M.O. & Sardin, M. (2007). Characterization of sulphate sorption on Callovo-Oxfordian argillites by batch, column and through-diffusion experiments. Physics and Chemistry of the Earth 32, 552–558.

Bhatti, J.S., Foster, N.W. & Evans, L.J. (1997). Sulphate sorption in relation to properties of podzolic and brunisolic soils in northeastern Ontario. Canadian Journal of Soil Science 77, 397–404.

Bradbury, M.H. & Baeyens, B. (1998). A physicochemical characterisation and geochemical modelling approach for determining porewater chemistries in argillaceous rocks. Geochimica et Cosmochimica Acta 62, 783–795.

Burzan, N. (2021). Growth and viability of microorganisms in bentonite and their potential activity in deep geological repository environments. Thesis 8002, EPFL Ecole Polytechnique Federale de Lausanne, Lausanne, 212 p.

Chao, T.T., Harward, M.E. & Fang, S.C. (1964a). Iron or aluminum coatings in relation to sulfate adsorption characteristics of soils. Soil Science Society of America Journal 28, 632–635.

812 Chao, T.T., Harward, M.E. & Fang, S.C. (1964b). Anionic effects on sulfate adsorption by
813 soils. Soil Science Society of America Journal 28, 581–583.

814 Charlet, L., Dise, N. & Stumm, W. (1993). Sulfate adsorption on variable charge soil and
815 reference minerals. Agriculture, Ecosystems & Environment 47, 87–102.

816 Charlet, L., Alt-Epping, P., Wersin, P. & Gilbert, B. (2017). Diffusive transport and reaction
817 in clayrocks: A storage (nuclear waste, CO_2, H_2), energy (shale gas) and water quality
818 issue. Advances in Water Resources 106, 39–59.

819 Chen, Y., Glaus, M.A., Van Loon, L.R. & Mäder, U. (2018). Transport of low molecular
820 weight organic compounds in compacted illite and kaolinite. Chemosphere 198, 226–237.

821 Claypool, G. E., Holser, W. T., Kaplan, I. R., Sakai, H., & Zak, I. (1980). The age curves of
822 sulfur and oxygen isotopes in marine sulfate and their mutual interpretation. Chemical
823 Geology, 28, 199–260.

824 Comfort, S.D., Dick, R.P. & Baham, J. (1992). Modeling soil sulfate sorption characteristics.
825 Journal of Environmental Quality 21, 426–432.

826 Courdouan, A., Christl, I., Meylan, S., Wersin, P. & Kretzschmar, R. (2007). Characterization
827 of dissolved organic matter in anoxic rock extracts and in situ porewater of the Opalinus
828 Clay. Applied Geochemistry 22, 2926–2939.

829 Debure, M., Tournassat, C., Lerouge, C., Madé, B., Robinet, J. C., Fernández, A.M. &
830 Grangeon, S. (2018). Retention of arsenic, chromium and boron on an outcropping clay-
831 rich rock formation (the Tégulines Clay, eastern France). Science of the Total
832 Environment 642, 216–229.

833 De Craen, M., Wang, L., Van Geet, M. & Moors, H. (2004). Geochemistry of Boom Clay
834 pore water at the Mol site. SCK-CEN Scientific Report BLG-990. Waste & Disposal
835 Department SCK-CEN, Mol, Belgium.

836 De Haller, A., Mazurek, M., Spangenberg, J. & Möri, A. (2014). SF (Self-sealing of faults
837 and paleo-fluid flow): Synthesis report. Mont Terri Technical Report, TR 2008-02, 63 pp.
838 Federal Office of Topography (swisstopo), Wabern, Switzerland.

839 Descostes, M., Blin, V., Bazer-Bachi, F., Meier, P., Grenut, B., Radwan, J., Schlegel, M.L.,
840 Buschaert, S., Coelho, D. & Tevissen, E. (2008). Diffusion of anionic species in callovo-
841 oxfordian argillites and oxfordian limestones (Meuse/Haute–Marne, France). Applied
842 Geochemistry 23, 655–677.

843 Fichtner, V., Strauss, H., Immenhauser, A., Buhl, D., Neuser, R.D. & Niedermayr, A. (2017).
844 Diagenesis of carbonate associated sulfate. Chemical Geology 463, 61–75.

845 Freivogel, M. & Huggenberger, P. (2003). Modellierung bilanzierter Profile im Gebiet Mont
846 Terri – La Croix (Kanton Jura). In: Heitzmann, P., Tripet, J.P. (Eds.), Mont Terri Project
847 – Geology, Paleohydrogeology and Stress Field of the Mont Terri Region, Federal Office
848 for Water and Geology Rep., vol. 4. Bern, Switzerland, pp. 7–44.

849 Fuller, R.D., David, M.B. & Driscoll, C.T. (1985). Sulfate adsorption relationships in forested
850 spodosols of the northeastern USA. Soil Science Society of America Journal 49, 1034–
851 1040.

852 Füchtbauer, H. (1988). Sedimente und Sedimentgesteine. Schweizerbart
853 Verlagsbuchhandlung, Stuttgart, 1141 p.

854 Gaines, G.L. & Thomas, H.C. (1953). Adsorption studies on clay minerals II. A formulation
855 of the thermodynamics of exchange adsorption. Journal of Chemical Physics 21, 714–
856 718.

857 Gaucher, E. C., Tournassat, C., Pearson, F. J., Blanc, P., Crouzet, C., Lerouge, C. & Altmann,
858 S. (2009). A robust model for pore-water chemistry of clayrock. Geochimica et
859 Cosmochimica Acta 73, 6470–6487.

860 Guadalix, M.E. & Pardo, M.T. (1991). Sulphate sorption by variable charge soils. Journal of
861 Soil Science 42, 607–614.

862 Gimmi, T. & Alt-Epping, P. (2018). Simulating Donnan equilibria based on the Nernst-
863 Planck equation. Geochim. Cosmochim. Acta 232, 1–13.

864 Huclier-Markai, S., Landesman, C., Rogniaux, H., Monteau, F., Vinsot, A. & Grambow, B.
865 (2010). Non-disturbing characterization of natural organic matter (NOM) contained in

clayrock porewater by mass spectrometry using electrospray and atmospheric pressure chemical ionization modes. Rapid Communications in Mass Spectrometry 24, 191–202.

Huclier-Markai, S., Monteau, F., Fernández, A., Vinsot, A. & Grambow, B. (2018). Natural organic matter contained in clayrock porewater: Direct quantification at the molecular level using electrospray ionization mass spectrometry. Rapid Communications in Mass Spectrometry 32, 1331–1343. https://doi.org/10.1002/rcm.8175.

Inskeep, W.P. (1989). Adsorption of sulfate by kaolinite and amorphous iron oxide in the presence of organic ligands. Journal of Environmental Quality 18, 379–385.

Jenni, A., Aschwanden, L., Lanari, P., de Haller, A., Wersin, P. (2019). Spectroscopic investigation of sulphur-containing minerals in Opalinus Clay. Nagra NAB 19-23. Nagra, Wettingen, Switzerland.

Kizcka, M., Wersin, P., Zwahlen, C. & Mäder, U. (2023). Porewater composition in clay rocks explored by advective displacement and squeezing experiments. Applied Geochemistry.

Krouse, H.R. & Mayer, B. (2000). Sulphur and oxygen isotopes in sulphate, in P.G. Cook & A.L. Herczeg (eds.), Environmental tracers in subsurface hydrology, New York, Springer, 195–231.

Lerouge, C., Grangeon, S., Claret, F., Gaucher, E.C., Blanc, P., Guerrot, C., Flehoc, C., Wille, G. & Mazurek, M. (2014). Mineralogical and isotopic record of diagenesis from the Opalinus Clay formation at Benken, Switzerland: Implications for the modeling of pore-water chemistry in a clay formation. Clays and Clay Minerals, 62, 286–312.

Lerouge, C., Maubec, N., Wille, G., Flehoc, C. (2015). GD experiment: Geochemical data experiment. Analysis of carbonate fraction in Opalinus Clay. Mont Terri Technical Note 2014-92.

Matusik, J. (2014). Arsenate, orthophosphate, sulfate, and nitrate sorption equilibria and kinetics for halloysite and kaolinites with an induced positive charge. Chemical Engineering Journal 246, 244–253.

Mayer B., Feger K.H., Giesemann A & Jaeger H.J. (I995). Interpretation of sulfur cycling in two catchments in the Black Forest (Germany) using stable sulfur and oxygen isotope data. Biogeochem. 30, 31–58.

Mazurek, M. (2017). Gesteinsparameter-Datenbank Nordschweiz – Version 2. In: Nagra Arbeitsbericht NAB, vols. 17–56. Wettingen, Switzerland.

Mazurek, M., Alt-Epping, P., Bath, A., Gimmi, T., Waber, H.N., Buschaert, S., De Cannière, P., De Craen, M., Gautschi, A., Savoye, S. & Vinsot, A. (2011). Natural tracer profiles across argillaceous formations. Applied Geochemistry 26, 1035–1064.

Mazurek, M. & de Haller, A. (2017). Pore-water evolution and solute-transport mechanisms in Opalinus Clay at Mont Terri and Mont Russelin (Canton Jura, Switzerland). Swiss Journal of Geosciences, 110, 129–149.

Mazurek, M., Aschwanden, L., Camesi, L., Gimmi, T., Jenni, A., Kiczka, M., Mäder, U., Rufer, D., Waber, H.N., Wanner, P., Wersin, P. & Traber, D. (2021). TBO Bülach-1-1: Data Report – Dossier VIII Rock properties, porewater characterisation and natural tracer profiles. Nagra Arbeitsbericht NAB 20-08.

Mazurek, M., Gimmi, T., Zwahlen, C., Aschwanden, L., Gaucher, E., Kiczka, M., Rufer, D., Wersin, P., Marques-Fernandes, M., Glaus, M., Van Loon, L., Traber, D., Schnellmann, M. & Vietor, T. (2023). Swiss deep drilling campaign 2019–2022: Geological overview and rock properties with focus on porosity and pore geometry. Applied Geochemistry.

Mäder, U. (2018). Advective displacement method for the characterisation of porewater chemistry and transport properties in claystone. Geofluids 2018, Article ID 8198762, doi.org/10.1155/2018/8198762

Müller, H., & Leupin, O. (2012). WS-H (Investigation of wet spots): Observation, first experimental results, and a short presentation of possible hypotheses regarding the origin of these waters. Mont Terri Technical Note, TN 2012-96, 49 pp. Federal Office of Topography (swisstopo), Wabern.

Nagra (2002). Project Opalinus Clay - Safety Report, Nagra Technical Report NTB 02-05. Nagra, Wettingen, Switzerland.

Parkhurst, D.L. & Appelo, C.A.J. (2013). Description of input and examples for PHREEQC version 3: A computer program for speciation, batch-reaction, one-dimensional transport, and inverse geochemical calculations. No. 6-A43. US Geological Survey.

Pearson, F.J., Arcos, D., Bath, A., Boisson, J.-Y., Fernández, A.M., Gäbler, H.-E., Gaucher, E., Gautschi, A., Griffault, L., Hernán, P., Waber, H.N. (2003). Mont Terri Project – Geochemistry of water in the Opalinus Clay Formation at the Mont Terri Rock Laboratory. swisstopo, Federal Office of Water and Geology.

Pekala, M., Wersin, P., Rufer, D. (2018). GD experiment: Geochemical data experiment. Mineralogy of carbonate and sulphate minerals in the Opalinus Clay and adjacent formations. Mont Terri Technical Report 2018-03.

Pekala, M., Smith, P., Wersin, P., Diomidis, N. & Cloet, V. (2020). Comparison of models to evaluate microbial sulphide generation and transport in the near field of a SF/HLW repository in Opalinus Clay. Journal of Contaminant Hydrology, 228, 103561.

Rao, S.M. & Sridharan, A. (1984). Mechanism of sulfate adsorption by kaolinite. Clays and Clay Minerals 32, 414–418.

Sadeghalvad, B., Khorshidi, N., Azadmehr, A., & Sillanpää, M. (2021). Sorption, mechanism, and behavior of sulfate on various adsorbents: A critical review. Chemosphere 263, 128064.

Thoenen, T., Hummel, W., Berner, U. & Curti, E. (2014). The PSI/Nagra chemical thermodynamic database 12/07. Paul Scherrer Institute, PSI Bericht Nr. 14-04. ISSN 1019-0643.

Tosco, T., Tiraferri, A. & Sethi, R. (2009). Ionic strength dependent transport of microparticles in saturated porous media: Modeling mobilization and immobilization phenomena under transient chemical conditions. Environmental Science & Technology, 43, 4425–4431.

Van Stempvoort, D.R., Reardon E.J. & Fritz P. (1990). Fractionation of sulfur and oxygen isotopes in sulfate by soil sorption. Geochim. Cosmochim. Acta 54, 2817–2826.

948 Waber, H.N., Gaucher, E.C., Fernández, A.M. & Bath., A. (2003). Aqueous Leachates and
949 Cation Exchange Properties of Mont Terri Claystones. In F.J. Pearson et al. (2003): Mont
950 Terri Project - Geochemistry of Water in the Opalinus Clay Formation at the Mont Terri
951 Rock Laboratory. Reports of the Federal Office of Water and Geology (FOWG), 185
952 Geology Series No 5. Federal Office of Topography (swisstopo), Wabern, Switzerland.

953 Waber, H.N. & Rufer, D. (2017). Porewater Geochemistry, Method Comparison and Opalinus
954 Clay-Passwang Formation Interface Study at the Mont Terri URL. Mont Terri Project,
955 Technical Report TR-2017-02. Nuclear Waste Management Organization NWMO,
956 Toronto, Canada.

957 Wersin, P., Mazurek, M., Waber, H.N., Mäder, U.K., Gimmi, T., Rufer, D. & de Haller, A.
958 (2013). Rock and porewater characterisation on drillcores from the Schlattingen borehole.
959 Nagra Arbeitsbericht NAB 12-54. Nagra, Wettingen, Switzerland.

960 Wersin, P. & Pękala, M. (2017). GD experiment: Geochemical Data experiment – Scoping
961 calculations for "CO2 experiment": Batch calculations and reactive transport modelling.
962 Mont Terri Technical Note TN 2017-21. Nagra, Wettingen, Switzerland.

963 Wersin, P., Pękala, M., Mazurek, M., Gimmi, T., Mäder, U., Jenni, A., Rufer, D. &
964 Aschwanden, L. (2020). Porewater chemistry of Opalinus Clay: Methods, Data,
965 Modelling & Buffering Capacity. Nagra Technical Report NTB 18-01. Nagra, Wettingen,
966 Switzerland.

967 Wersin, P., Mazurek, M., Gimmi, T. (2022). Porewater chemistry of Opalinus Clay revisited:
968 Findings from 25 years of data collection at the Mont Terri Rock Laboratory. Applied
969 Geochemistry 138, 105234.

970 Wynn, P.M., Fairchild, I.J., Borsato, A., Spötl, C., Hartland, A., Baker, A., Frisia, S. &
971 Baldini, J.U. (2018). Sulphate partitioning into calcite: Experimental verification of pH
972 control and application to seasonality in speleothems. Geochimica et Cosmochimica Acta,
973 226, 69–83.

974 Zwahlen, C., Gimmi, T., Jenni, A., Kizcka, M., Mazurek, M., Van Loon, L. & Mäder, U.
975 (2023). Chloride accessible porosity fractions across the Jurassic sedimentary rocks of
976 northern Switzerland. Applied Geochemistry.

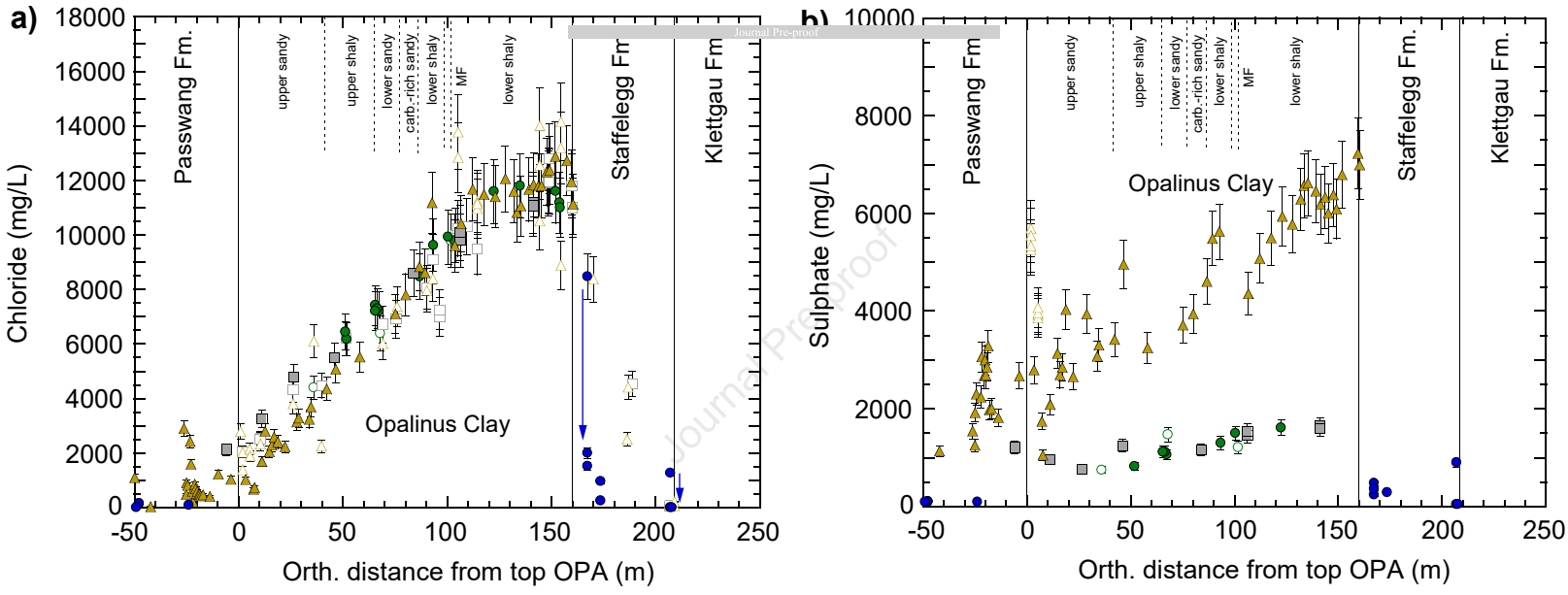
a)
b)
Chloride (mg/L)
Sulphate (mg/L)
Orth. distance from top OPA (m)
Passwang Fm.
upper sandy
upper shaly
lower sandy
carb.-rich sandy
lower shaly
MF
lower shaly
Staffelegg Fm.
Klettgau Fm.
Opalinus Clay
Borehole waters (Pearson et al., 2003)
Borehole waters (newer data)
Leachates (Person et al., 2003)
Leachates (newer data)
Squeezed waters (Pearson et al., 2003)
Squeezed waters (newer data)
Groundwaters & seepages

a)

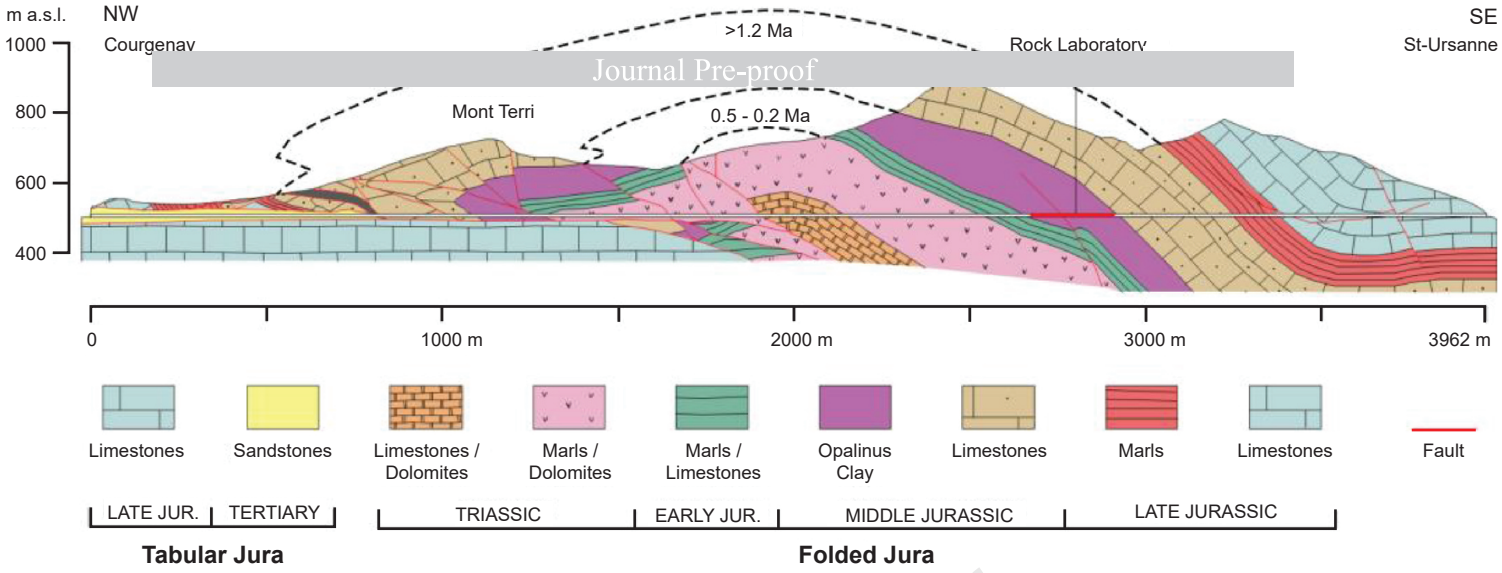

b)

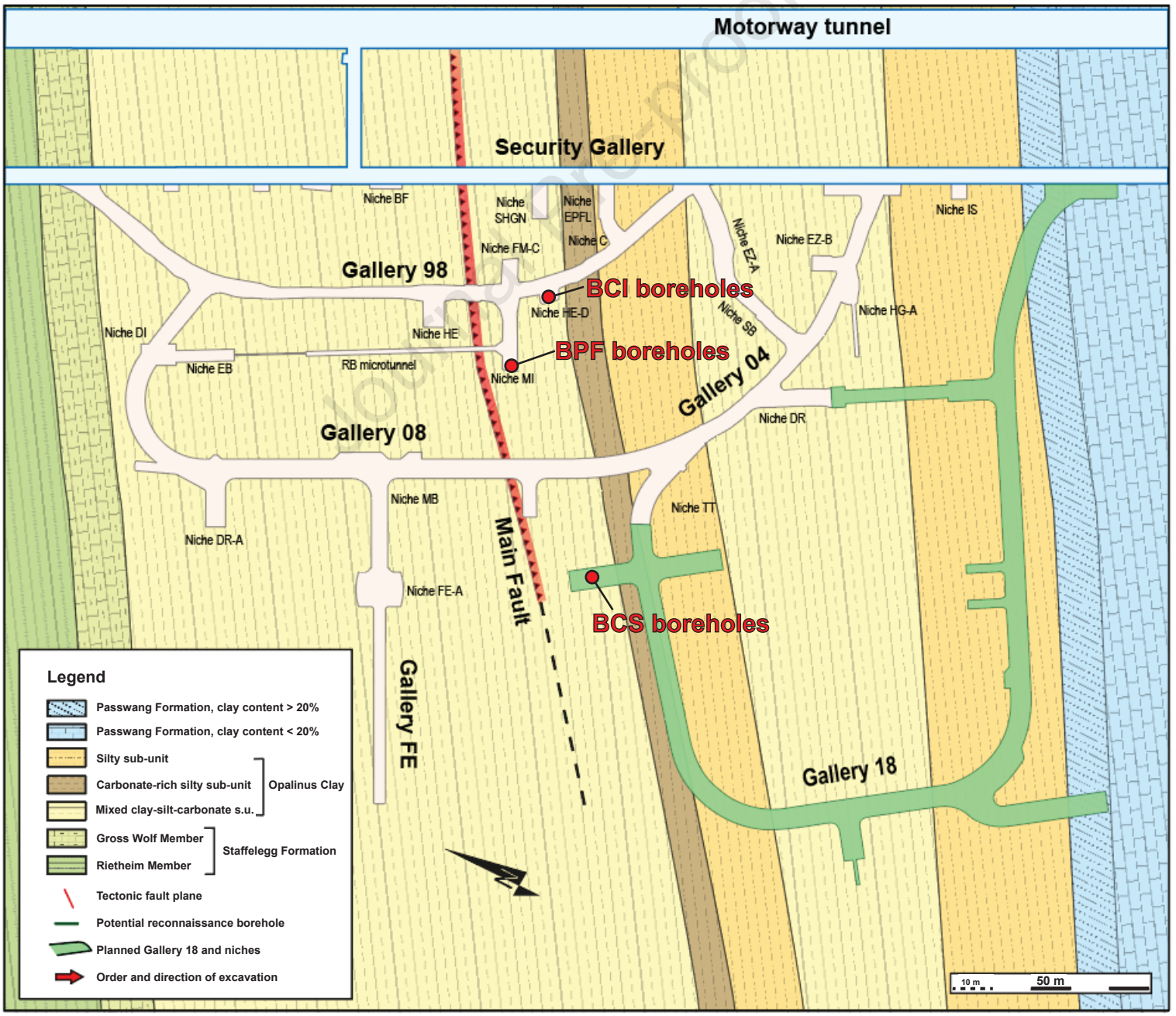

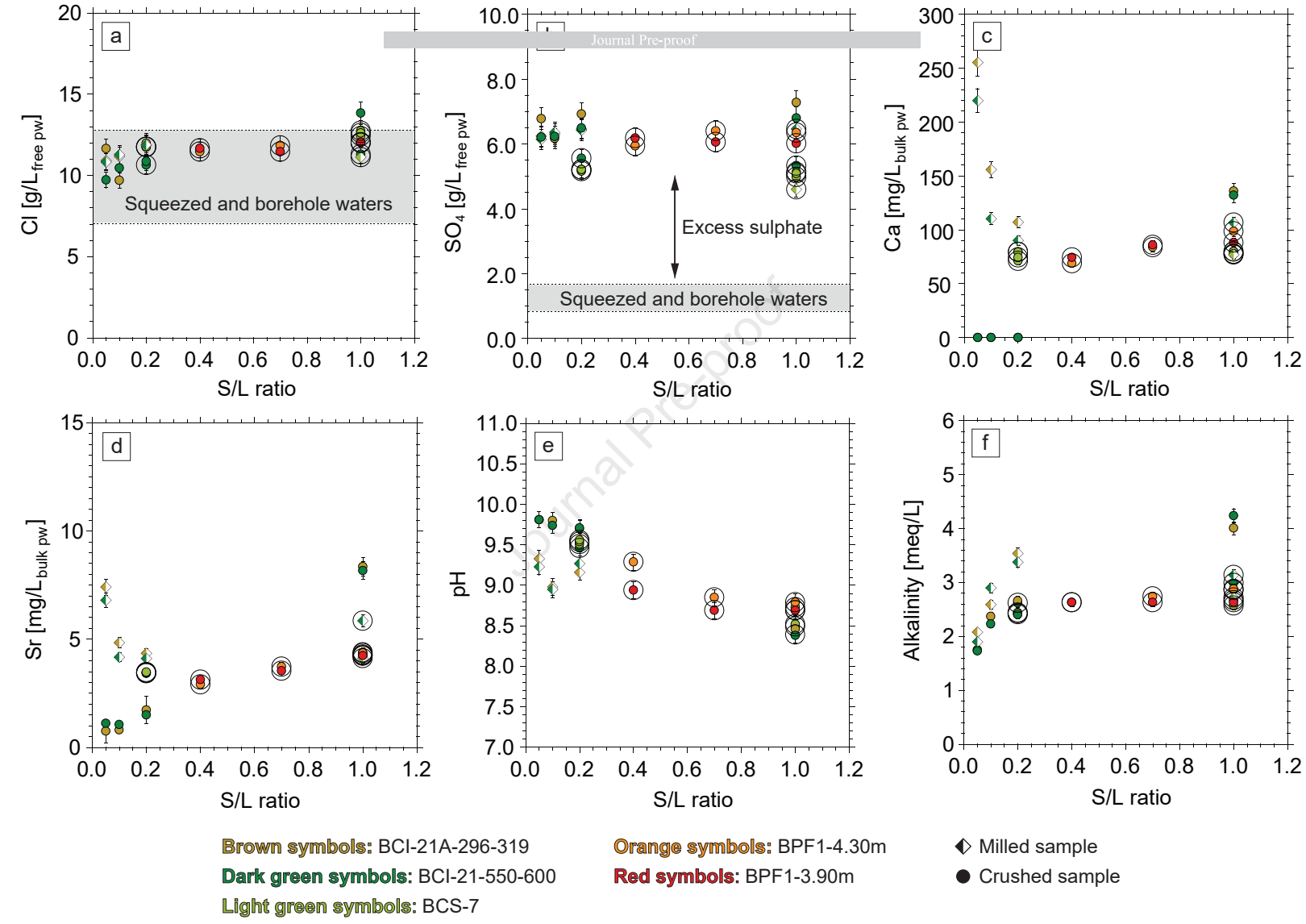

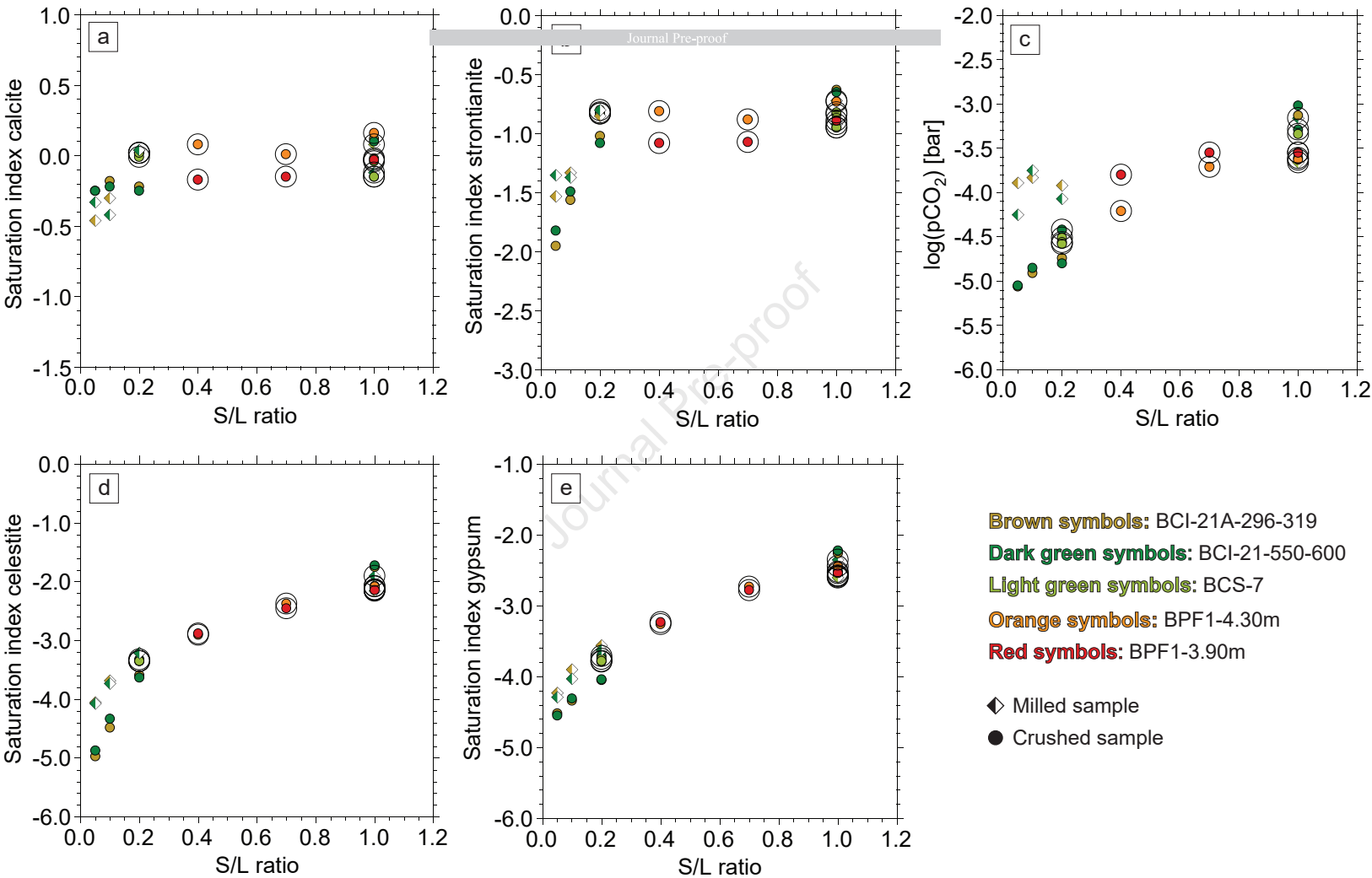

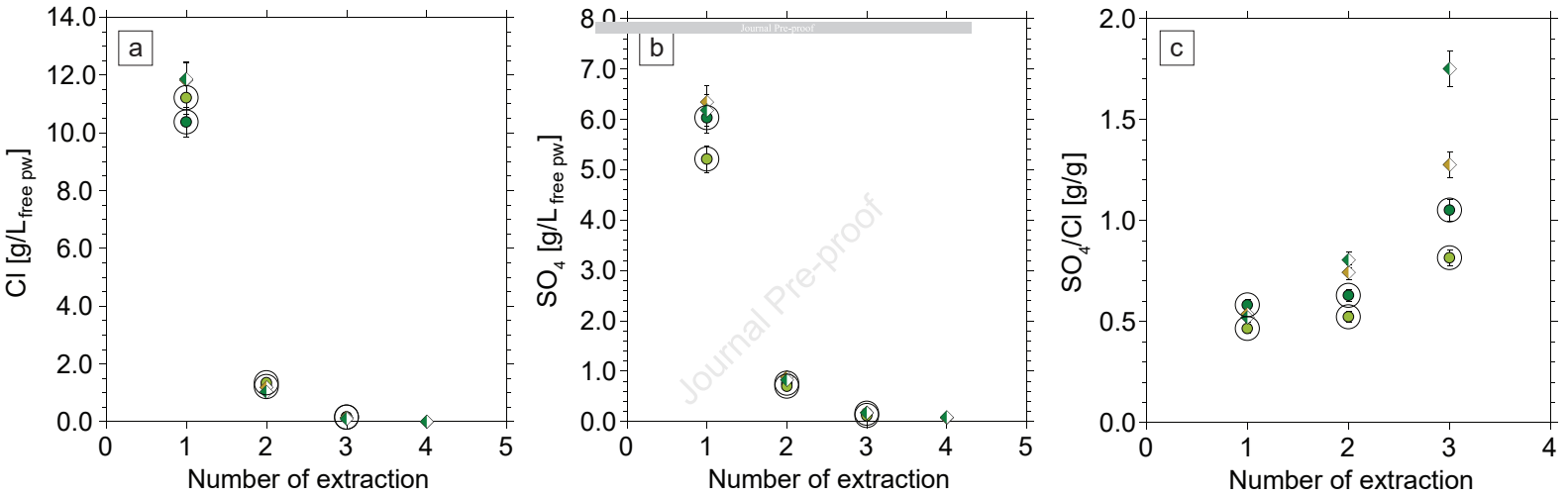
a
Cl [g/L free pw]
Number of extraction
b
SO4 [g/L free pw]
Number of extraction
c
SO4/Cl [g/g]
Number of extraction
Journal Pre-proof
Brown symbols: BCI-21A-296-319
Dark green symbols: BCI-21-550-600
Light green symbols: BCS-7
Milled sample
Crushed sample

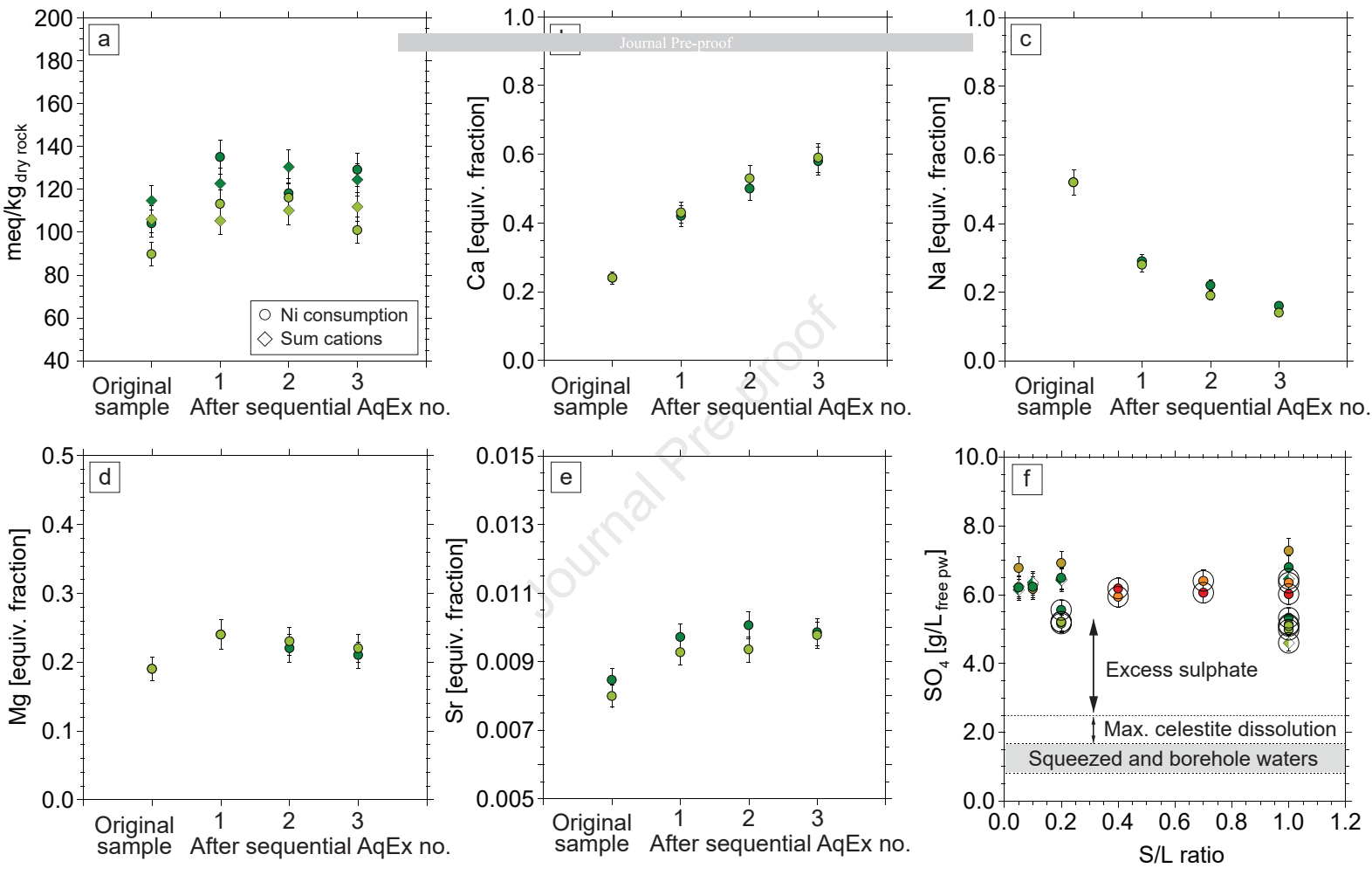

Brown symbols: BCI-21A-296-319
Dark green symbols: BCI-21-550-600
Light green symbols: BCS-7
Orange symbols: BPF1-4.30m
Red symbols: BPF1-3.90m
Milled sample
Crushed sample

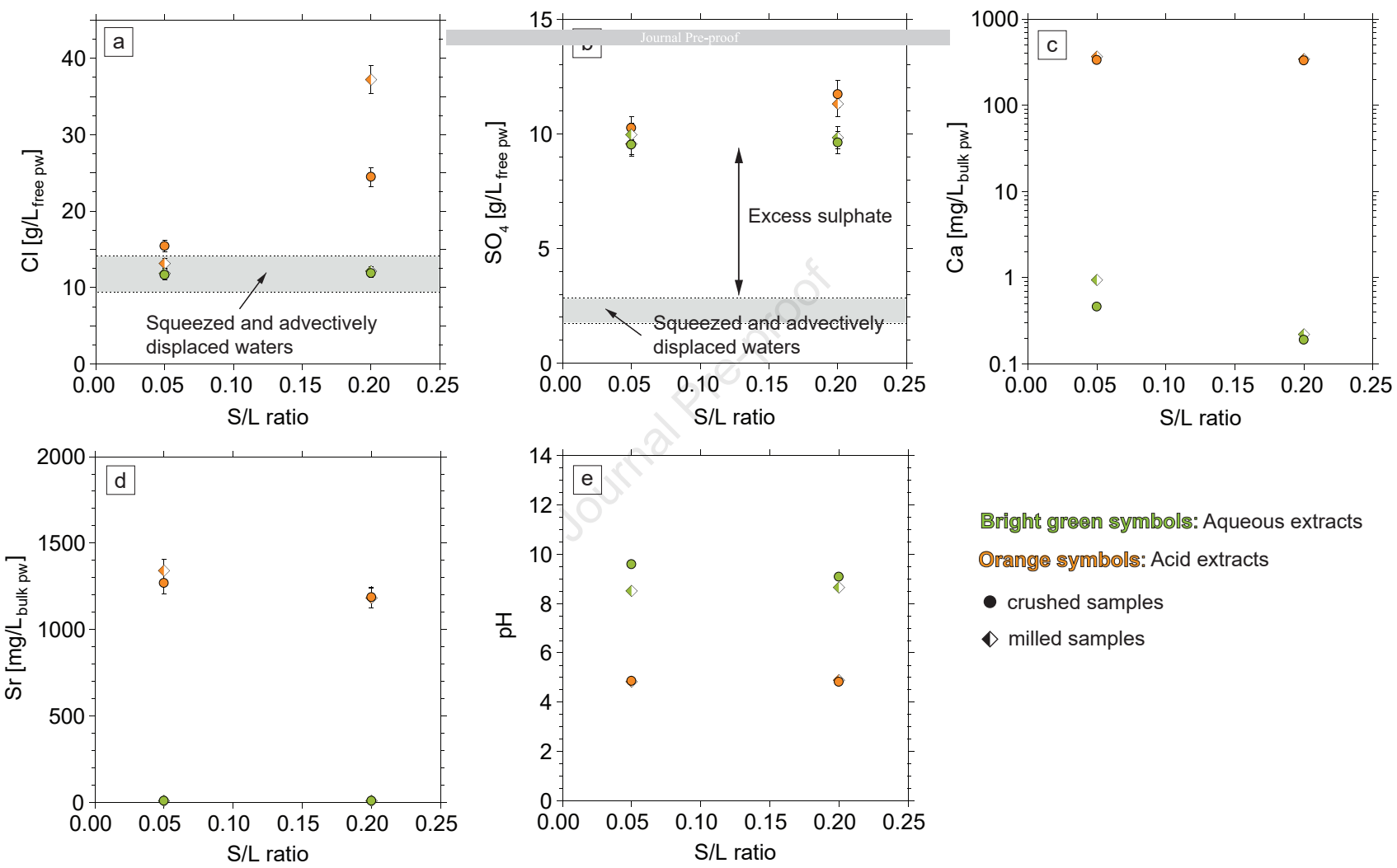

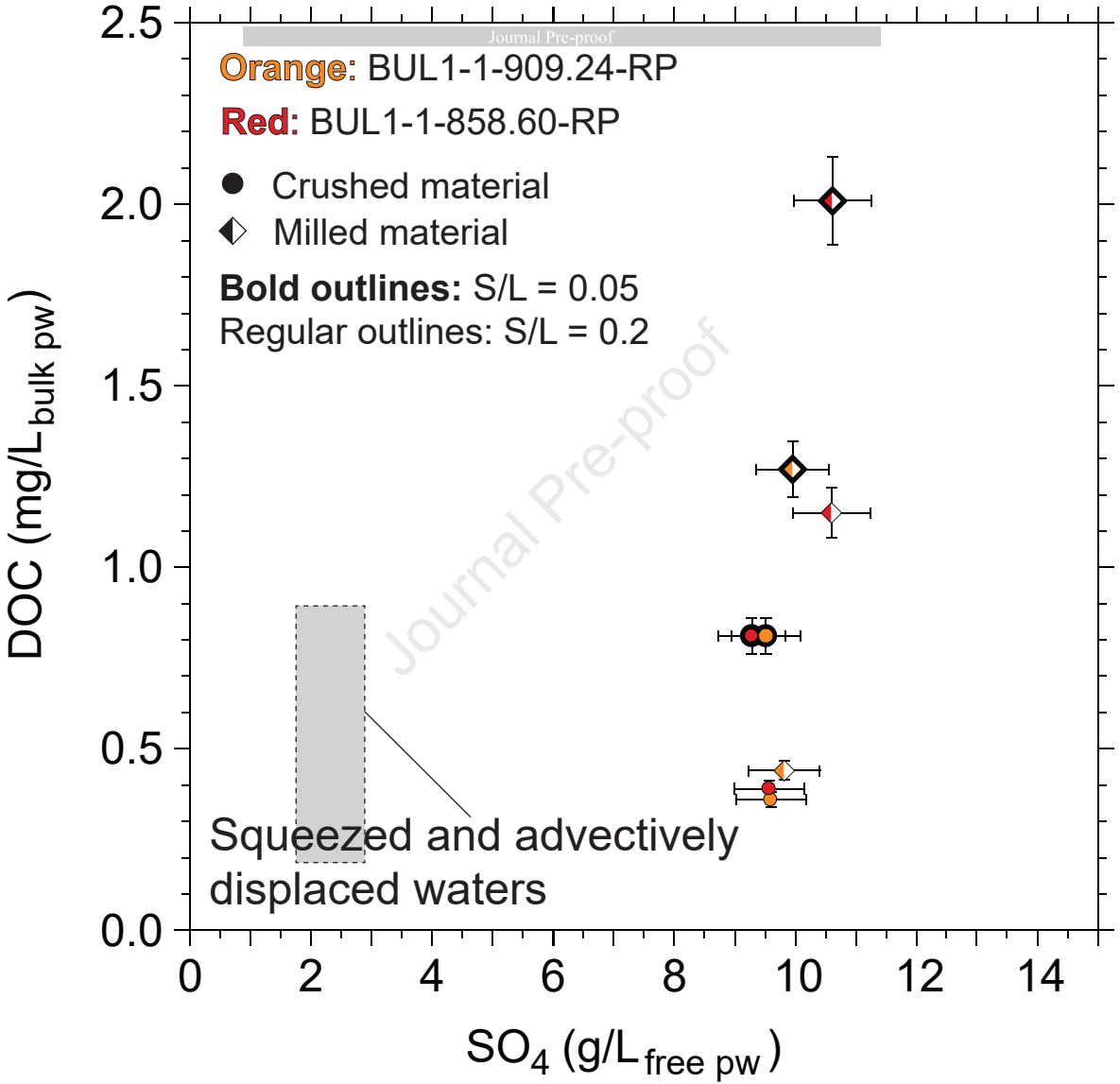

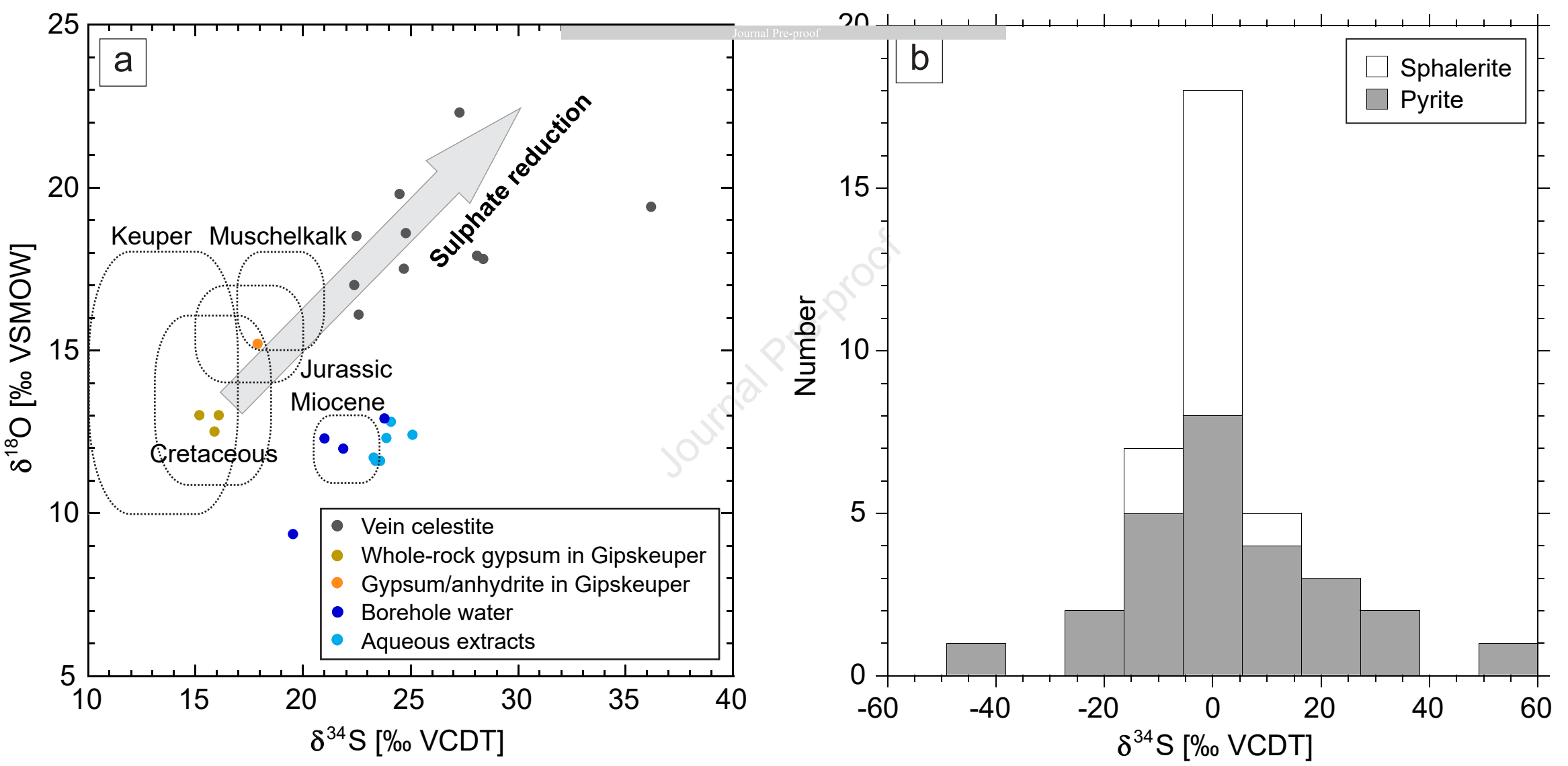

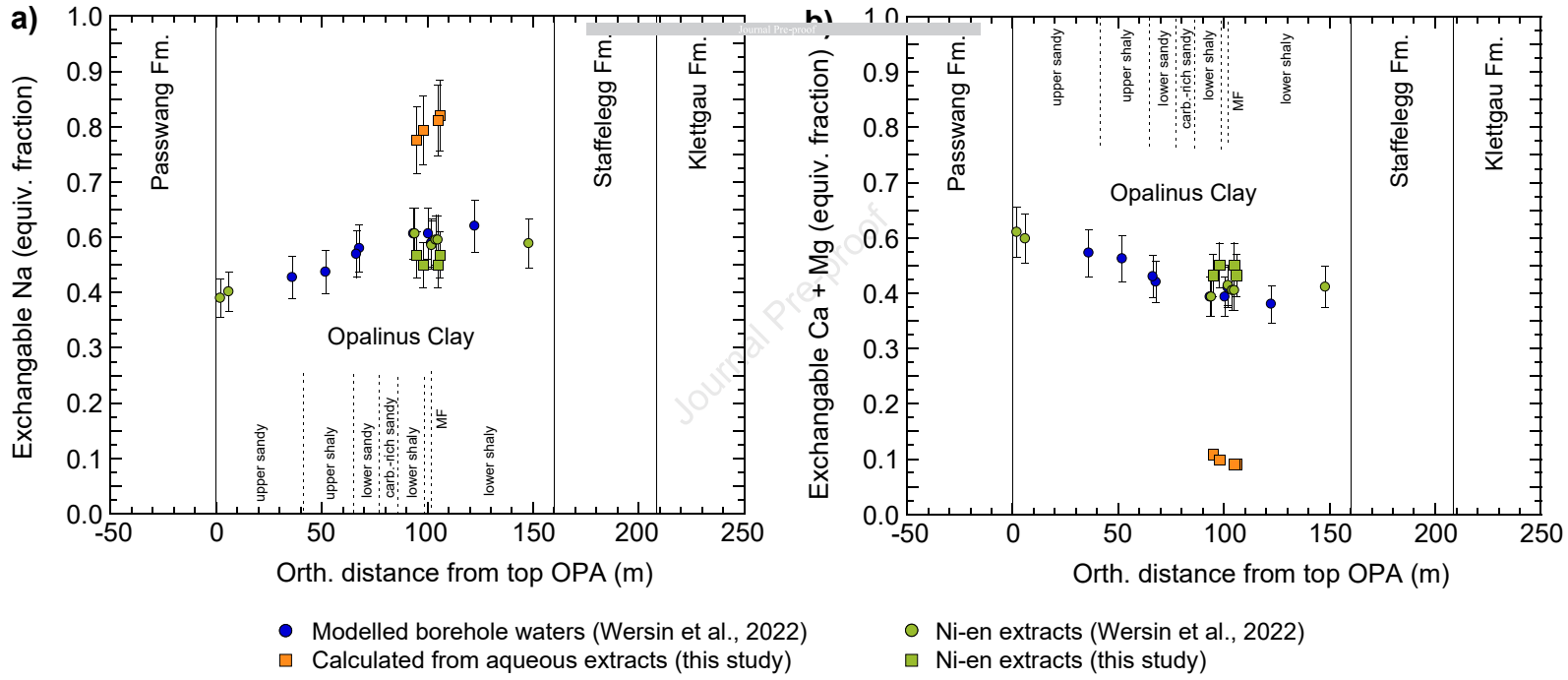

Highlights

- Excess SO_4 in aqueous extracts of Opalinus Clay samples
- Experimental study of water-extractable sulphate in Opalinus Clay
- Obvious sulphate sources fail to explain excess SO_4 in aqueous extracts
- Dissolved SO_4 in aqueous extracts and borehole water is isotopically similar
- Possibly, some sulphate is weakly bound to mineral surfaces

Declaration of interests

☒ The authors declare that they have no known competing financial interests or personal relationships that could have appeared to influence the work reported in this paper.

☐ The authors declare the following financial interests/personal relationships which may be considered as potential competing interests: